Applying MCMusf

for

Evaluating the spatial and temporal dynamics of the Jordan River water quality

Shai Arnon and Eilon Adar

Ben-Gurion University of the Negev

Draft

2013

Jordan River Basin Water Management Research Project

Table of contents

1 Introduction

1.1 General background

The Lower Jordan River Basin (JRB) between the Sea of Galilee and the Dead Sea is a long (~100 Km) and narrow depression that is part of the Syrian–African Rift system (Figure 1). The Jordan River drops about 200 m along the entire basin length (from -212 at the outlet of the Sea of Galilee to -416 m below the sea level in the Dead Sea), and divide the basin to the eastern side (Hashemite Kingdom of Jordan) and the western side (Israel and the Palestinian Authority). The actual meandering length of the river is about 250 km, which drains an area of approximately 15,000 km^2.

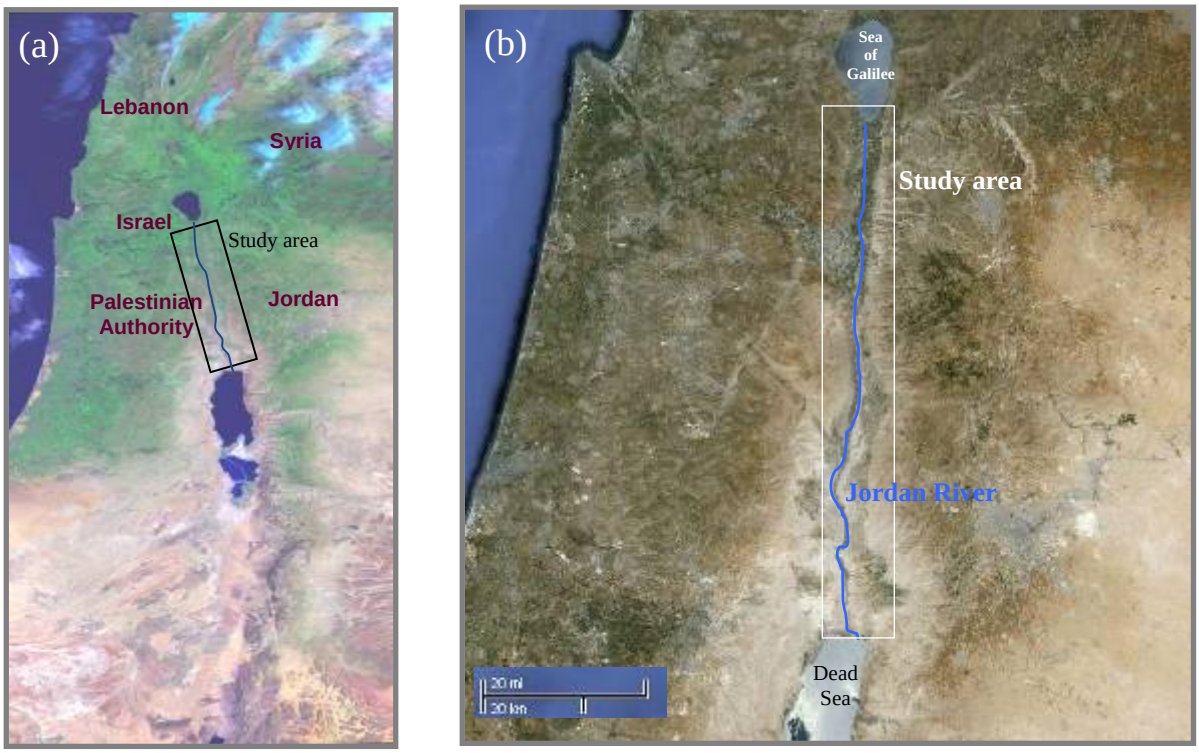

Figure 1: The study area (marked as a rectangle) shown on a Satellite images of the 5 riparian's sharing the Jordan River tributaries (a) and the Lower Jordan River Basin (b).

The climate in the Lower Jordan River Basin (JRB) is characterized by hot, dry summer with high daily fluctuations and cool winter with short transitional seasons. Rainfall occurs mainly during the winter months (November – May), with average precipitation sharply declining from about 400 mm/year near the Sea of Galilee to < 100 mm/year near the Dead Sea (Figure 2).

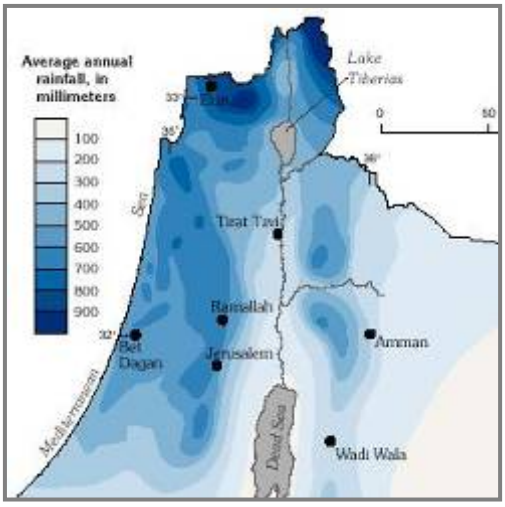

Figure 2: Average annual rainfall in the region of the study area (http://exact-me.org/overview/images/p04_map.gif)

Presence of people and agriculture activity in the JRB dates back 10,000 of years. Because of water availability from the Jordan River, micro climate and the fertile soils deposited as sediments originated from by frequent floods, the JRB has been extensively used for food production. In the last century, water allocation projects (e.g., King Abdullah Canal in the eastern side of the river), greenhouse technologies, and advanced irrigation techniques have increased the agricultural production, which is largely exported outside of the JRB. Today, about 150,000 inhabitants live along the valley, with an estimated number of 85,000 people on the Jordanian side and 68,000 on the western side of the river (50,000 Palestinians and 18,000 Israelis). Most of

these people still rely on agriculture as the main source of income. However, further development in the JRB, and even the last of the current agricultural activity, is questionable as consequences of diminishing water quantity and the deterioration of the water quality along the basin.

1.2 Water resources management and future development in the Jordan River Basin

The water in the JRB is withdrawn from surface water systems, such as the King Abdullah Canal and from subsurface reservoirs (aquifers) along the foothills of the mountains ridges. Until the middle of the 20th century, the Jordan River discharged about 1300 million cubic meters per year (MCM/yr) to the Dead Sea (Salameh & Naser, 1999), and was used as the main source of available water for the lower Jordan River region. However, massive diversion of water from the vast Jordan basin by Israel, Jordan and Syria led to a decline of the Jordan River discharge to the Dead Sea to a total of only 30–200 MCM/yr (Efrat Farber, et al., 2007; Holtzman, et al., 2005). Today, the outlet of the Sea of Galilee into the lower Jordan River is dammed at Deganiya and Alumot, and the flow of the Yarmouk River is attenuated at the Adassiya Dam. Downstream of the dams, only poor-quality water currently discharges to the Jordan River (Abu-Jaber & Ismail, 2003; Efrat Farber, et al., 2007; Holtzman, et al., 2005; Moller, et al., 2007; Rosenthal, Guttman, Sabel, & Moller, 2009). Additional relatively small streams drain to the Jordan River, mainly from the eastern escarpment of the rift. Also, effluents from fish ponds and agriculture return flows as well as wastewater reach the Jordan River along its flow path, contributing relatively small amount of water with low quality (Anker, Rosenthal, Shulman, & Flexer, 2009;

E. Farber, et al., 2005). The aforementioned drastic changes in hydrological regime within the JRB, resulted in a complex dynamic interaction in terms of water quantities and qualities between the different surface and groundwater systems, where each water body can serve as a source or a sink, while the Jordan River reflects the mixing between all sources (Abu-Jaber & Ismail, 2003; Al-Jayyousi & Bergkamp, 2008; Al Kuisi, Aljazzar, Rude, & Margane, 2008; E. Farber, et al., 2005).

As for typical cross-borders water sources, it is clear that Israeli, Palestinian and Jordanian domestic and agriculture water in the JRB are linked and will continue to be so in the future. Today, contaminants from both sides of the Jordan River Basin are leached into groundwater bodies that some leaks and seep into the Jordan River Basin, as well as into the Jordan River itself. There is no immediate agreed solution to remediate the Jordan River and to increase water allocation along the valley. The various types of effluents and the groundwater seepage into the Jordan River elevated its salinity and modified its chemical composition (Abu-Jaber & Ismail, 2003; Al-Jayyousi & Bergkamp, 2008; Al Kuisi, et al., 2008; E. Farber, et al., 2005). Nutrients, fertilizers, pesticides and herbicides deteriorated the Jordan Water quality with direct impact on the aquatic ecology (Al-Jayyousi & Bergkamp, 2008; Barel-Cohen, et al., 2006; Segal-Rozenhaimer, et al., 2004). Therefore, in order to develop the region, one needs to understand the current hydrological and hydro-chemical situation in order to find solutions for the Jordan River remediation and to improve the Jordan River Basin water management. Water management is also critical to maintain current activities because water quality is constantly degrading (Al-Jayyousi & Bergkamp, 2008; E. Farber, et al., 2005). The anticipated expansion of wastewater

treatment by all partners, as well as the relative contribution of wastewater to the river, calls for understanding the potential benefit and risks associated with the use of treated wastewater to replace the withdrawal of fresh water from the Jordan River. This project elaborates on the current active water sources, identifies and quantifies the sources of contaminants into the Jordan River. Finally, it describes the critical research needs, and demonstrates the way to achieve the Jordan River remediation in order to allow new sustainable development with acceptable environmental impact in the JRB.

1.3 Objectives

In order to cope with the lack of available data on the hydrological system, we need to evaluate and integrate our current knowledge, which was gathered from disparate research and monitoring programs, within one framework of analysis. Collecting and analyzing the entire hydro-chemical datasets will enable us to achieve the main goal of this study, namely to **evaluate the water quality dynamics along the Jordan River as a function of anthropogenic activities and natural processes. It is aimed to provide a basis for remediation and sustainable development of the Jordan River Basin**.

Within the framework of our main goal, the specific objectives of our study were to:

- Collect the existing spatial and temporal water quality data in the Jordan River Basin (streams, drains, shallow groundwater, seeping water, natural water sources, effluents and potential sources of water contaminants).
- Identifying all potential water contributors to the Jordan River.
- Collect the data on fluxes along the Jordan River and of its tributaries.

- Demonstrate the applicability of the MCM modeling approach to quantify current water quantities (associated with its qualities) in order to provide a scientific based platform to be used for the assessment of the future development of the Jordan River Basin.
- Facilitate partnerships with academic and governmental institutions in the region to form a regional research group for a long term study on the water resources in the Jordan River Basin.

2 Methods

The main tool that we used in this study is known as the Mixing Cell Modeling (MCM) approach. The MCM is proposed to unveil the largely obscured groundwater contribution and to quantify the fluxes of contaminated groundwater into rivers and lakes systems in order to assess the cause for water quality deterioration and the damage to the aquatic systems. This provided us with the unique opportunity to quantitatively assess the flows of specific contaminants into water bodies and to elaborate the natural chemical evolution along the groundwater movement and along the river.

2.1 Work plan

The work plan of this study consists of 2 main phases:

Phase 1- The first phase of this research involved data collection on the quality of various water bodies contributing to the water resources of Jordan River Basin, as well as the discharge fluxes of the various sources. All was based on data from peer-reviewed journals, published and unpublished reports, and personal exchange of information with other scientists working in this region. Maps and satellite images were used to identify the natural and anthropogenic contaminated sources endangering the water quality of the Jordan River. This includes, selecting representative hydro-chemical settings along the Jordan River including the following features: local groundwater reservoir contributing to the base flow of the Jordan River, selected aquifers (groundwater bodies such as mountain front recharge, shallow groundwater, and tile drainage) that might replenish or seeps into the Jordan

River and/or its tributaries. All the data is now organized in a unified database which enabled a comprehensive data processing of both, spatial and temporal distribution of all available hydro-chemical parameters.

Phase 2- In this part of our work we conducted rigorous data processing and model simulations to identify gaps and missing data, as well as to provide proof of concept. This phase was the core section of this work. We applied the MCM approach, developed by Adar et al. (1992), to quantify the 3 dimensional interaction of surface water and subsurface water units. The MCM was advanced recently into a user-friendly code for the quantitative assessment and definition of groundwater flow patterns in multiple-aquifer flow systems by environmental tracers of dissolved minerals and isotopes. The MCM has been developed for complex aquifer systems in basins with scarce hydrological information. The model was applied in several hydrological basins worldwide, from the Kalahari Desert (Namibia), Jezreel and Bessor basins (Israel), to the Ili basin in Kazakhstan. A novel MCM approach was developed also for transient flow systems, and applied in the Arava aquifer of Jordan and Israel in order to define the transient groundwater flow system and the relative groundwater contribution from Jordanian and Israeli sources.

2.2 Mixing Cell Modeling

The mixing cell modeling approach has been developed for complex geological systems with vague sub-surface hydrological pattern and scarce hydrological information. It has also been adopted to identify and quantify sources of pollutants flowing and seeping into flow pattern along streams and resolve the spatial distribution and evolution of dissolved contaminants along complex configuration of

streams and rivers. Much of the deterioration of water quality along streams and within lakes aquatic systems is caused by sources of contaminants that enter water bodies from various tributaries and seepage of ground water sources, some of which are point sources and others are relatively diffused. Most are "hidden" and hard to locate and identify geographically. On top of this, the relative water discharge from each source and therefore the accurate amount of contaminants are hard to assess quantitatively. The spatial distribution of various sources of pollutants along rivers and lakes is closely related to the spatial distribution and relative contribution of each of the active sources of water recharge. Dealing with ground water and surface water resources combined with the anthropogenic impact (industry and agriculture), creates a complex hydrological and hydrochemical system which is difficult to model and therefore almost impossible to assess quantitatively. For these kinds of complex hydrological systems, MCM approach offers an attractive solution.

In a complex hydrological systems the boundaries, and hydrological conditions along the boundaries, are not sufficiently clear or distinct, and there is a lack of sufficient hydro-geological and hydro-chemical information. Thus, it is difficult to construct, solve and calibrate a hydrological model based on the continuity approach. The MCM allows the hydrological modeling of mass transfer of water including both naturally dissolved minerals and anthropogenic pollutants and dissolved contaminants in the aquatic system. The MCM algorithm is based on a more simplistic approach in which the flow domain is sub- divided into pseudo- homogeneous flow cells forming a multi-compartmental flow model. The creation of the multi-compartmental structure is based on spatial (and temporal, for unsteady flow) distribution of dissolved ions and

isotopes in the hydrological system. The modeled flow system (river basins or aquifers) is subdivided into homogeneous compartments within which all the considered parameters are assumed to be constant for a specific time period, such as hydraulic heads and solute concentrations, including isotopic composition. Mixing of various sources or contributors (such as from upstream compartments and external sources) and dilution with water already existing in the cell control the concentration of the characteristic chemicals and/or the isotopic compositions of each compartment. Therefore, every well-mixed or homogeneous aquifer section (cell or compartment) is characterized by a unique representative chemical concentration and/or isotopic composition. Water balance and dissolved salt balance expressions in terms of mass flux of water the dissolved minerals and contaminants are composed for every cell and among the cells within the flow domain.

2.3 Assessment of groundwater fluxes by environmental traces

The MCM_{sf} (Mixing Cell Model for Steady Flow system) enables the calculation of groundwater fluxes and assessing the contribution from various sources in a complex, yet steady hydro-geological system in which the spatial distribution of dissolved minerals are stable/constant with time.

A set of balance equations for the flux of water and for the associated flux of solutes is written for each cell n over a given time period dt. For a simplified flow model of water with a constant density the mass balance for the cell n is expressed by the following equation:

$$(1)\quad \sum_{r=1}^{R_n} Q_{rn} + \sum_{i=1}^{I_n} q_{in} - \sum_{j=1}^{J_n} q_{nj} - W_n = S_n \frac{dh_n}{dt}$$

The symbol Q_{rn} denotes *R* different unknown sources into cell *n*, and q_{in} denotes the (unknown) flux from the i^{th} upstream compartment or cell into the n^{th} cell. In the above example of a schematic compartmental flow system, for *cell I*, I = 0 (no internal fluxes from upstream cells), and there are 3 external sources, r = 1, 2 and 3. In a similar way, q_{nj} stands for the outflow from the n^{th} cell into the j^{th} cell. W_n accounts for withdrawal of water from *cell n*, i.e. a sink term or pumping rate in the n^{th} cell. The inflows and outflows are iterated over the number of inflows, *I*, and the number of outflows, *J*, into each cell. S_n represents the storage capacity within *cell n* and h_n denotes the hydraulic head associated with that cell.

For a steady flow system or for quasi-steady flow over a sufficiently long time interval, an average water balance expression is obtained:

$$(2)\quad \sum_{r=1}^{R_n} \overline{Q}_{rn} + \sum_{i=1}^{I_n} \overline{q}_{in} - \sum_{j=1}^{J_n} \overline{q}_{nj} - \overline{W}_n = \varepsilon_n$$

The notations are the same as in Equation 1 except that each term represents the average fluxes for the specific time interval designated with top-bars. An error term ε_n is introduced in order to account for any error associated with either measurements or assessment of the flow system and other deviations from flux balance in cell *n*.

For a quasi-steady state variation of the dissolved constituents, the mixing cell concept is applied, based on mass balance expressions for each tracer *k* (k = 1, 2,…, K) in cell *n*:

$$(3)\quad \sum_{r=1}^{R}\overline{C_{rk}Q_{rn}}+\sum_{i=1}^{I}\overline{C}_{ink}\overline{q_{in}}-\overline{C}_{nk}\left[\sum_{j=1}^{J}\overline{q}_{nj}+\overline{W}_n\right]=\varepsilon_{nk}$$

$\overline{C_{rk}Q_{rn}}$ denotes the average flux of the k^{th} constituent from source r into cell n. $\overline{q_{in}}$ represents the average flux from the i^{th} cell into the n^{th} cell, having an average concentration $\overline{C_{ink}}$ of solute k. In Equation 3, $\overline{C_{nk}}$ denotes the concentration of the k^{th} constituent within cell n and $\overline{q_{nj}}$ stands for the average outflow from the nth cell into the j^{th} one. The average pumping from the n^{th} cell during a specific time interval is expressed by $\overline{W}_n$, and ε_{nk} is the error associated with the mass balance of the k^{th} constituent or the deviation from the solute balance in cell n. For every cell n, there are K+1 equations: one for the water balance and K more for every k species (k=1,2,.....,K). This is demonstrated in Equation 4.

$$(4)\quad \begin{aligned}
&\sum_{r=1}^{R_n}\overline{Q}_{rn}+\sum_{i=1}^{I_n}\overline{q}_{in}-\sum_{j=1}^{J_n}\overline{q}_{nj}-\overline{W}_n=\varepsilon_n\\
&\sum_{r=1}^{R}\overline{C_{rk_1}Q_{rn}}+\sum_{i=1}^{I}\overline{C}_{ink_1}\overline{q_{in}}-\overline{C}_{nk_1}\left[\sum_{j=1}^{J}\overline{q}_{nj}+\overline{W}_n\right]=\varepsilon_{nk_1}\\
&\sum_{r=1}^{R}\overline{C_{rk_2}Q_{rn}}+\sum_{i=1}^{I}\overline{C}_{ink_2}\overline{q_{in}}-\overline{C}_{nk_2}\left[\sum_{j=1}^{J}\overline{q}_{nj}+\overline{W}_n\right]=\varepsilon_{nk_2}\\
&\sum_{r=1}^{R}\overline{C_{rk_3}Q_{rn}}+\sum_{i=1}^{I}\overline{C}_{ink_3}\overline{q_{in}}-\overline{C}_{nk_3}\left[\sum_{j=1}^{J}\overline{q}_{nj}+\overline{W}_n\right]=\varepsilon_{nk_3}\\
&\quad\vdots\qquad\qquad\vdots\qquad\qquad\vdots\qquad\qquad\vdots\\
&\sum_{r=1}^{R}\overline{C_{rK}Q_{rn}}+\sum_{i=1}^{I}\overline{C}_{inK}\overline{q_{in}}-\overline{C}_{nK}\left[\sum_{j=1}^{J}\overline{q}_{nj}+\overline{W}_n\right]=\varepsilon_{nK}
\end{aligned}$$

Upon combining Equations 2 and 3 into a matrix form for each cell n, the following is obtained:

$$\underline{\underline{C}}_n \underline{X}_n + \underline{P}_n = \underline{E}_n \quad (5)$$

where $\underline{\underline{C}}_n$ is a matrix with known concentrations in cell *n*,

$$\underline{\underline{C}}_n = \begin{bmatrix} 1, & 1, & \cdots, 1, & 1, & 1, & \cdots, 1, & -1, & \cdots, -1 \\ \overline{C}_{r_1 nk_1}, & \overline{C}_{r_2 nk_1}, & \cdots, & \overline{C}_{Rnk_1}, & \overline{C}_{i_1 nk_1}, & \overline{C}_{i_2 nk_1}, & \cdots, \overline{C}_{Ink_1}, & -\overline{C}_{nk_1}, \cdots, -\overline{C}_{nk_1} \\ \overline{C}_{r_1 nk_2}, & \overline{C}_{r_2 nk_2}, & \cdots, & \overline{C}_{Rnk_2}, & \overline{C}_{i_1 nk_2}, & \overline{C}_{i_2 nk_2}, & \cdots, \overline{C}_{Ink_2}, & -\overline{C}_{nk_2}, \cdots, -\overline{C}_{nk_2} \\ \vdots & \vdots & \vdots & \vdots & \vdots & \vdots & \vdots & \vdots \\ \overline{C}_{r_1 nK}, & \overline{C}_{r_2 nK}, & \cdots, & \overline{C}_{RnK}, & \overline{C}_{i_1 nK}, & \overline{C}_{i_2 nK}, & \cdots, \overline{C}_{InK}, & -\overline{C}_{nK}, \cdots, -\overline{C}_{nK} \end{bmatrix}_{[(K+1)\bullet(R_n+I_n+J_n)]} \quad (6)$$

$\underline{X}_n$ is a vector of the unknown fluxes through the boundaries of cell *n*, $\underline{P}_n$ is a vector containing elements with known values in cell *n* (such as known fluxes of pumping) and $\underline{E}_n$ is the error vector in cell *n* presented in equations (7), (8) and (9) respectively.

$$\underline{X}_n = \begin{bmatrix} \overline{Q}_{r_1} \\ \overline{Q}_{r_2} \\ \vdots \\ \overline{Q}_{R_n} \\ \overline{q}_{i_1} \\ \overline{q}_{i_2} \\ \vdots \\ \overline{q}_{I_n} \\ \overline{q}_{nj_1} \\ \overline{q}_{nj_2} \\ \vdots \\ q_{nJ_n} \end{bmatrix}_{[(R_n+I_n+J_n)\bullet 1]} \quad (7)$$

$$(8)\quad P_n = \begin{bmatrix} \overline{W}_n \\ \overline{C}_{nk_1}\overline{W}_n \\ \overline{C}_{nk_2}\overline{W}_n \\ \overline{C}_{nk_3}\overline{W}_n \\ \vdots \\ \overline{C}_{nK}\overline{W}_n \end{bmatrix}_{[(K+1)\bullet 1]} \qquad (9)\quad \underline{E}_n = \begin{Vmatrix} \varepsilon_n \\ \varepsilon_{nk_1} \\ \varepsilon_{nk_2} \\ \varepsilon_{nk_3} \\ \vdots \\ \varepsilon_{nK} \end{Vmatrix}_{[(K+1)\bullet 1]}$$

Based on equation (5) and by assembling the square error terms over all cells we obtain a quadratic objective function (10):

$$(10)\quad J = \sum_{n=1}^{N} \left[\underline{E}^T \underline{\underline{\Phi}}\, \underline{E}_n\right] = \sum_{n=1}^{N} \left[(\underline{\underline{C}}_n \underline{X}_n + \underline{P}_n)\Phi(\underline{\underline{C}}_n \underline{X}_n + \underline{P}_n)\right]$$

where ^{T} denotes transpose and $\underline{\underline{\Phi}}$ represents a diagonal matrix comprising weighting values about estimated errors (independent of each other) expected for each of the terms, which compose the mass balance for the fluid and the dissolved constituents. The weighting matrix $\underline{\underline{\Phi}}$ also reflects the degree of confidence to which the tracers are assumed conservative and/or the degree of accuracy of the analyses. For further elaboration on Equations 1 to 9, the reader is referred to Adar et al. (1988; 1988) and Adar and Sorek (1989).

The total flux components in the aquifer can now be estimated by minimizing the sum of square error, J. All flux components in the aquifer can now be estimated by a minimization of the square error sums J. Similar to a procedure suggested by Adar and Sorek (1989), by virtue of Equation 5 with the modified vector $\underline{X}_n$ (Equation 15) and by assembling the square error terms over all N cells we obtain a quadratic objective function similar to Equation 10. The large set of water and mass balance

equations serve as linear constraints in the optimization scheme, which is the selection of the "most suitable" solution out of a large number of possible solutions. Quadratic programming solution based on Wolf Algorithm is proposed for quantitative evaluation of recharge and subsurface fluxes for a multi-aquifer system under steady flow conditions.

As a result of the mathematical optimization, a flow rate is attributed to each potential flow connection. Depending on the results obtained from the mathematical optimization, the flow model might be changed by modification of the proposed flow pattern and potential sources.

Repeated failures of a model optimization scheme indicate a complete disagreement between the hydrogeological and hydrochemical flow pattern versus the proposed set-up of the model. This implies the need for modification of the proposed compartmental flow pattern associated with a possible revision of the assigned set of potential contributors. In some cases, problems with model optimization even necessitate a review of the hydrogeological system analysis, i.e., the definition of compartments and possible flow and hydraulic connections among cells and suggested sources of recharge.

3. Results

3.1 Hydrological zones along the JRB

A hydro-chemical database based on all sources with relevant data from several sampling campaigns obtained by various projects was established and it now includes: 25 sampling locations along the Lower Jordan River; 20 inflows-streams, 7 springs, 3 fish ponds locations, 16 drains, and 27 boreholes from the western basins. The Hydro-chemical data from Eastern Basins include 38 inflows, 9 springs and groundwater samples from 10 boreholes. In addition, 4 locations along Wadi Faria stream were sampled for effluents (from raw sewage in the upper basin and mixture with fresh groundwater springs, downstream). All sampling locations are posted on a satellite image presented in Figure 3. While sampling locations along the Jordan River are designated by red squares, all the other potential sources are posted with blue symbols.

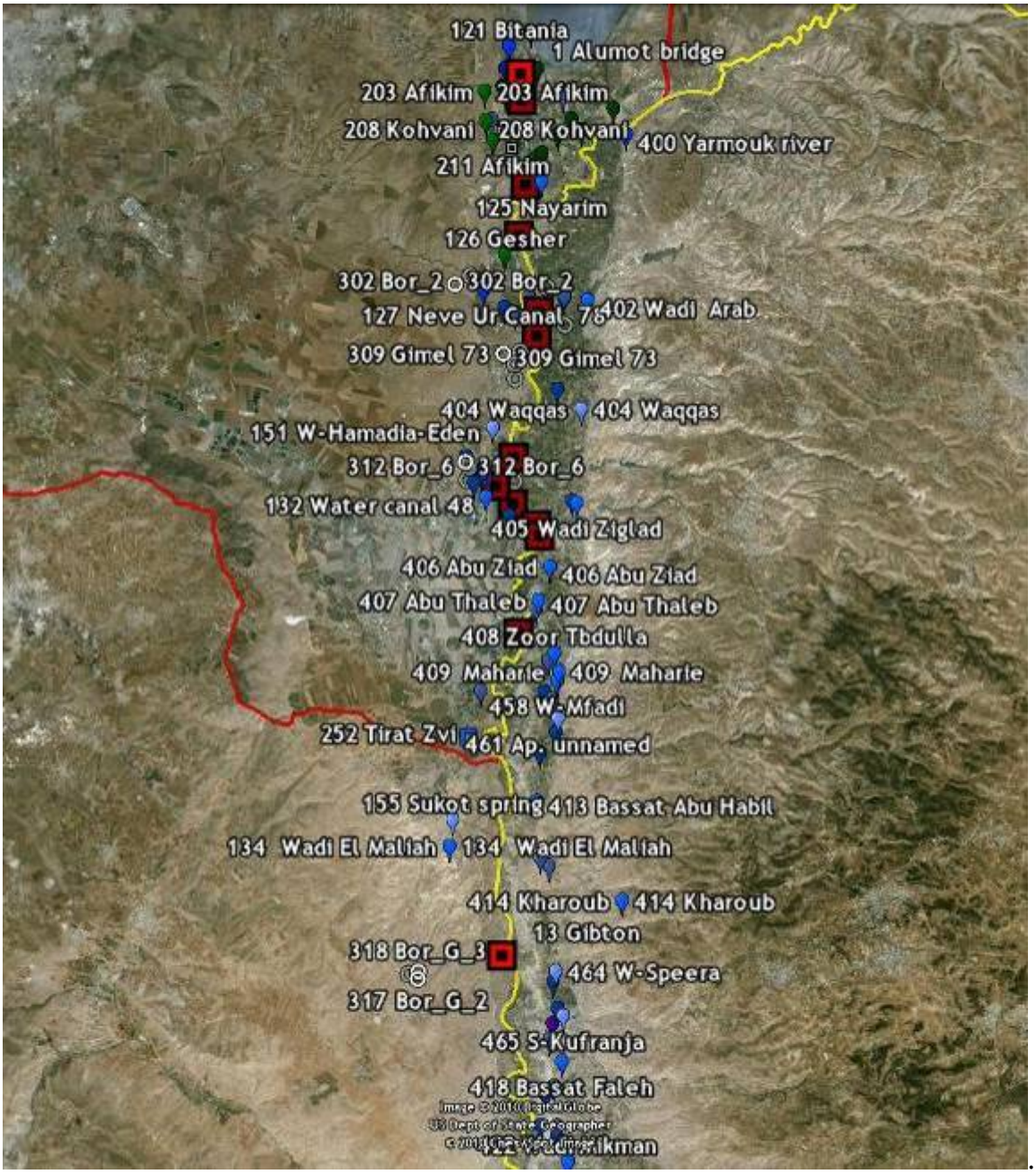

Figure 3. Water sampling locations along the Jordan River (red) and boreholes, springs, drains as potential sources of pollutants (all in blue).

The most comprehensive hydrochemical and isotopes data that encompasses the entire Jordan Valley is from four sampling campaigns performed in 2000-2001. The winter of 2000/2001 was extremely humid with rainfall amount far above the long term average over the Jordan River basin. That year, the Sea of Galilee reached its

full capacity and water was released to the lower Jordan River after many years that the dam was remained closed. Floods from the Yarmuk River and from smaller tributaries provided substantial runoff into the Lower Jordan River that washed down the contaminated – salty water and sediments and provided the river with clean fresh water after so many years. In addition, discharge into the Jordan River from springs and drains were noticed after many dry years. Therefore, we selected this data set to evaluate the flow pattern into the Jordan Valley under humid winter conditions and under extreme dry summer. Hydro-chemical data and isotopes from various locations along the Jordan Valley that were collected in the following years are also included in the data set to complete the hydro-chemical data base for missing information mainly for the summer dry period. The database includes information on the salinity, pH, temperature, concentrations of Ca^{2+}, Mg^{2+}, Na^{+}, K^{+}, Cl^{-}, SO_4^{2-}, HCO_3^{-}, NO_3^{-}, Br^{-}, B^{+}, Sr^{2+} and isotopes: $\delta^{11}B$, $^{87}Sr/^{86}Sr$, $\delta^{34}S_{sulfate}$, $\delta^{15}N_{nitrate,}$ $\delta^{18}O_{water}$.

The Jordan River system was divided into 20 compartments or segments following the assessment of the hydro-chemical and isotopes data. Due to incomplete data (mainly for the Eastern Jordan basin), potential external sources such as groundwater seepage from cultivated area (drains & boreholes) and water release from sewage treatment plants are assumed to provide similar "quality" of water all year around. We assume that these kind of potential sources contribute similar quality of water all year around. In addition, the following assumptions hold:

- The Jordan River gains water from various sources along the Jordan Valley from Sea of Galilee in the north to Dead Sea in the south: streams, seepage from

groundwater, leakage from irrigation (drains) and from point sources such as fish ponds and water treatment plants.

All potential sources and contributors have been identified and characterized for the hydro-chemical and isotopic composition.

The list of water sampling locations over the Lower Jordan Valley as posted in Figure 3 with reference to the distance from the Sea of Galilee (Alumot Bridge) is given in Table 1.

Table 1: List of sampling locations and their distance from Alumot Bridge.

Id	Name	Distance from Alumot
	Outlet of Sea of Galilee	0.0
W.Surf.Inflow_121	Bitaniya	0.0
	M.N.M (without the sewage)	0.0
W.Surf.Inflow_122	Saline carrier	0.0
W.Surf.Inflow_123	W. Yavneal	0.4
W.Drainage_200	Degania b- kav tet 1	1.0
W.Drainage_201	Beit Zera - Cowshed	1.7
W.Drainage_202	Robed	1.8
W.Drainage_203	Afikim	2.2
W.Drainage_204	Kelet -kav h	2.2
W.Drainage_205	Kochvani h1 (sewage)	2.2
W.Drainage_206	Point 121	2.6
W.Ground_207	Afikim - Groundwater	2.7
W.Drainage_208	kochvani	2.7
W.Drainage_209	Sha'ar hagolan	3.1
W.Drainage_210	Yarmuhim Reservoir	3.3
W.Drainage_211	Afikim	3.4
E.Surf.Inflow_400	Yarmouk River	3.5
W.Drainage_212	Point 110	3.7
W.Drainage_213	Ashdot waste	4.9
W.Drainage_214	Sephen Ashdot	5.0
W.Drainage_215	Zor- Ashdot	5.4
W.Surf.Inflow_125	Yarmuok River - Naharayim	6.3
W.Drainage_126	Gesher drainage (81)	10.7
E.Well_451	Igam well	10.8

W.Bor_301	Borehole 1	11.0
W.Bor_302	Borehole 2	11.2
W.Surf.Inflow_127	N.Ur - Water canal (78)	11.5
W.Bor_303	Shaar 78	11.6
W.Surf.Inflow_303	Shaar 78 River	11.6
W.FP_250	N.Ur pond	11.6
E.Surf.Inflow_401	North Shuna bridge	12.0
E.Ground_452	North Shuna thermal	12.0
E.Surf.Inflow_402	Wadi Arab	12.2
W.Surf.Inflow_128	N.Ur - Water canal (76)	12.2
W.Bor_304	Gimel 74	12.7
W.Surf.Inflow_129	N.Ur - Water canal (74)	12.7
W.Bor_304	Neve Ur South	12.7
E.Well_453	Fish F. well	13.0
W.Bor_308	Borehole 3	13.2
W.Bor_309	Gimel 73	13.2
W.Bor_310	Borehole 4	13.8
W.Bor_311	Borehole 5	13.8
E.Surf.Inflow_403	Wadi Teibeh	16.5
E.Surf.Inflow_404	Waqqas	17.6
W.Well_151	Hamadia - Well	18.2
W.Bor_312	Borehole 6	18.6
W.Bor_313	Borehole 7	18.6
W.Bor_314	Shaar 56 Doshen	18.6
W.Surf.Inflow_130	Hamadiya - south canal	18.9
W.FP_251	Fish pond Hamadiya	19.2
E.Spring_454	Manshiya thermal	19.2
W.Bor_324	Canal 56 gimel	19.5
E.Well_455	Waqqas well	19.7
W.Ground_152	En Huga (Soda Station)	20.4
W.Spring_153	Hasida Spring	20.4
W.Surf.Inflow_131	Harod	20.8
W.Surf.Inflow_132	Water canal 48	21.4
E.Surf.Inflow_405	Wadi Ziglab	21.9
W.Surf.Inflow_133	Water canal Nimrod	22.2
E.Surf.Inflow_406	Abu Ziad	23.4
E.Surf.Inflow_407	Abu Thableh	26.8
E.Spring_456	Sp. unnamed	27.1
E.Surf.Inflow_408	Zoor Tbdulla	28.5
E.Spring_457	Abu thableh spring	28.5
E.Surf.Inflow_409	Masharie	29.1
E.Surf.Inflow_458	Masharie	29.1
W.Spring_154	A-tin Spring	31.8
E.Surf.Inflow_410	Mahrab Abu Ahm.	31.8
W.Spring_459	Juneidi Sp.	32.2

E.Well_460	Zenati F. well	32.4
W.Spring_461	Sp. Unnamed	33.5
W.FP_252	Tirat Zvi - pools	33.5
E.Surf.Inflow_411	Bassat Sharhabil	34.1
E.Surf.Inflow_412	Yabis	36.4
E.Surf.Inflow_413	Bassat Abu Habil	36.9
W.Spring_155	Sukot Spring	37.4
W.Surf.Inflow_134	Wadi el maliach	38.1
W.Spring_462	Qarn Sp.	39.2
W.Spring_463	Abu Namroud Sp.	39.2
E.Surf.Inflow_414	Kharoub	43.2
W.Bor_316	Borhole G-1	
W.Bor_317	Borhole G-2	
W.Bor_318	Borhole G-3	
E.Spring_464	Speera Sp.	45.2
E.Surf.Inflow_415	Bassat Abu Hamid	45.9
E.Surf.Inflow_416	Bassat Al Amira	47.7
E.Spring_465	Kufranja Sp.	47.9
E.Surf.Inflow_417	Rajib Seebiya	49.0
E.Spring_466	Faleh Sp.	50.6
E.Surf.Inflow_418	Bassat Faleh Wadi Botton	51.5
E.Spring_467	Buweib Sp.	51.9
E.Surf.Inflow_419	Bweib	52.7
E.Surf.Inflow_420	El Kheil	54.0
E.Spring_468	Kafir Sp.	54.0
E.Surf.Inflow_421	Kafir	54.2
E.Spring_469	Sp. unnamed	54.4
E.Surf.Inflow_422	Wadi Mikman	55.3
E.Surf.Inflow_423	Twal (west) Hawaya	57.0
E.Well_470	Deir Alla thermal well	57.2
E.Surf.Inflow_424	Mifshel	58.8
E.Surf.Inflow_425	Bassat Shakran	59.7
W.Surf.Inflow_135	Rafultzik-zarzir south	59.7
W.Bor_315	Argaman swamp	63.0
E.Surf.Inflow_426	Zarqa River	66.3
W.Surf.Inflow_136	Tirtcha Upper	66.7
E.Surf.Inflow_427	Rasif	69.2
E.Bor_500	Damya Well no. 1	70.0
E.Surf.Inflow_428	Abu Mayyala	70.3
E.Surf.Inflow_429	Aqraa	70.3
E.Surf.Inflow_430	Mallah Gdeida	70.4
W.Ground_156	Tirtcha Groundwater	70.6
E.Surf.Inflow_431	Qurein pool	71.9
W.Bor_321	Borhole T-2	
W.Bor_322	Borhole T-3	

W.Bor_323	Borhole T-4	
W.Bor_320	Borhole T-1	
E.Surf.Inflow_432	Mallaha	72.5
W.Surf.Inflow_137	Tirtcha Lower	72.7
W.Surf.Inflow_138	Wadi el Ah'mar	75.0
E.Surf.Inflow_433	Bassat El Faras	80.1
E.Surf.Inflow_434	Wadi Mallaha Karama	80.9
Cell_d	Zur el mandase	84.6
W.Surf.Inflow_139	Uga Melecha	86.7
W.Ground_157	Uga Melecha-groundwater	86.7
E.Well_471	Wadi Kafrain well	96.2
W.Well_158	Hagla - Well	96.7
E.Well_472	Rama well	96.7
E.Surf.Inflow_435	Kharar	96.8
E.Well_473	Hisban well	98.7
E.Surf.Inflow_436	Hisban Kafrain	98.8

Further data analyses identified the basic hydrological units (also called "cells") to be used in the MCM (Table 2) and presented in Figure 3.

Table 2: List of sampling locations on the river and their distance from Alumot Bridge

Id	Name	Distance from Alumot (km)
Cell_1	Alumot Bridge	0.1
Cell_2	Beit Zera	1.3
Cell_3	Dalhamiya	5.6
Cell_4	Gesher	8.7
Cell_5	Neve Ur North	11.6
Cell_6	Neve ur - South	12.7
Cell_7	Hamadiya pump - North	18.4
Cell_8	Hamadiya pump - South	20.1
Cell_9	g-48	21.1
Cell_10	Maoz Haim	22.2
Cell_11	Sheich Husein Bridge	22.7
Cell_12	Shifa' Station	27.7
Cell_13	Gibton	44.0
Cell_14	Zarzir Station-58	59.7
Cell_15	Adam Bridge	66.4
Cell_16	Tovlan Station -83	72.4
Cell_17	Gilgal - 107	76.6
Cell_18	Alenby Bridge	91.4

Cell_19	Baptism site	95.6
Cell_20	Ab'dala Bridge	100.0

Based on the chemical and isotopic analysis, the JRB can be divided into three main hydrological zones (E. Farber, et al., 2004);

Zone 1- the northern section stretches 22 km downstream from the Sea of Galilee. This section is characterized by a decrease in chloride, calcium, and sodium concentrations and increase in magnesium and sulfate concentrations. Figures 4 and 5 display the longitudinal concentrations of chloride and sulfate during May and August, 2001.

Zone 2- A central section between 22–66 km downstream from the Sea of Galilee, where salt variations are minimal (Figures 4 and 5).

Zone 3- A southern section, 66–100 km downstream from the Sea of Galilee, in which the chloride and sulfate concentrations increase downstream, particularly during August (Figures 4 and 5).

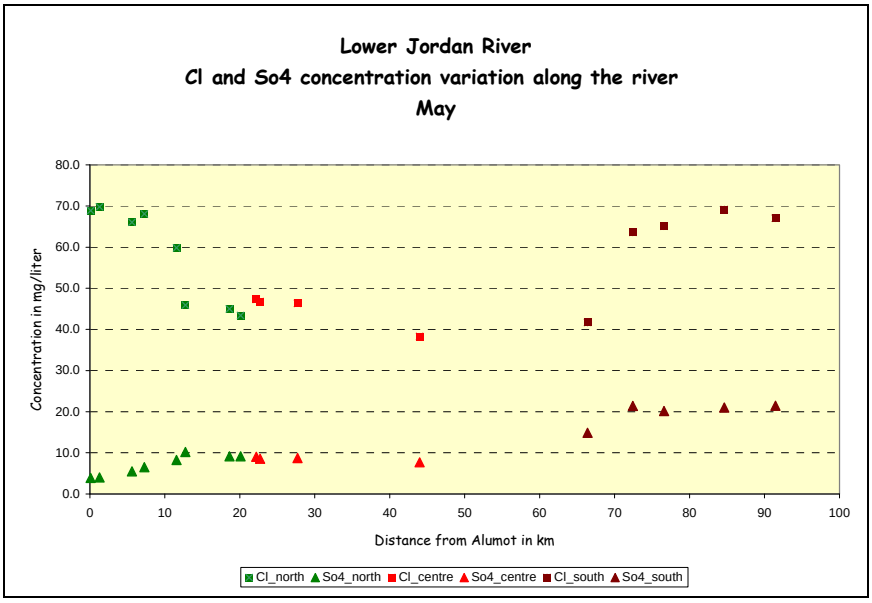

Figure 4. Variation of Cl and SO4 along the lower Jordan River – May

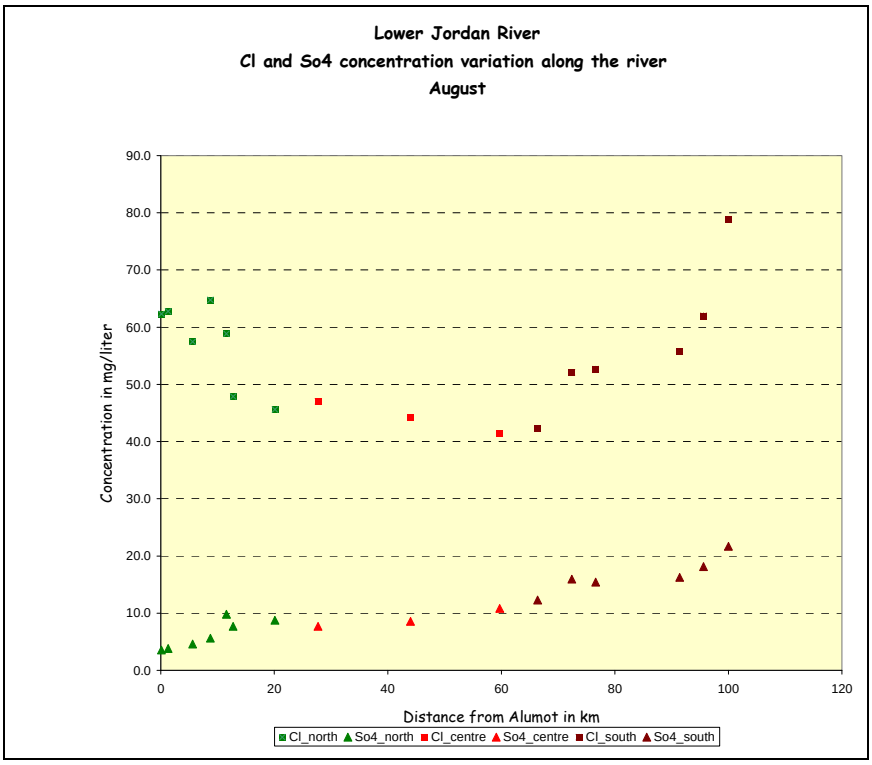

Figure 5. Variation of Cl^- and SO_4^{2-} along the lower Jordan River – August

3.2 MCM Results for single compartments/segments along the Lower Jordan Valley

The following MCM modeling analyses were performed on average chemical and isotopic data for the winter (September 2000-February 2001) and summer (March 2001-August 2001).

The results of MCM modeling analyses for single cell model are displayed in the following tables. In cases, where for some flow components, data is not available data for the specific period, average value is used (designated by *). Potential sources with incomplete hydro-chemical data are designated by **. *** designate cases where hydro-chemical data and even average values are missing for the specific required period. Existing hydro-chemical data with uncertain sampling date is marked with ****.

Cell 1: Results for the upper Jordan River at Alumot dam- Alumot Bridge (0.1 km from Alumot)

Winter 2001 was exceptionally humid and water from the Sea of Galilee was released through the Degania dam for few weeks.

Downstream to Alumot dam, the possible sources alimenting the Lower Jordan River are:

- Cell 0: in provenance of Sea of Galilee
- The saline 7 brines water carrier.
- Bitanya

In order to avoid increasing the salinity in the Sea of Galilee, the saline springs are deviated artificially by the 'Saline Water Carrier' to Alumot Dam. Sewage effluents from Tiberius are also diverted to the Jordan River via the 'Bitania Plant'. Agricultural sewage drained through 'Bitanya' pipe.

The saline water carrier that collects all saline springs that emerges at the western shore of the Sea of Galilee is characterized by low Na/Cl (.0.67) and SO4/Cl (0.06) ratios. Bitanya effluents have high Na/Cl (.0.895) and low SO4/Cl (.137).

The results (Table 3) of the single cell model show that all the three sources contribute to the salinity of the river water at the beginning of the Lower Jordan River.

Following the MCM results, the winter flux at Alumot is mixture of ~14.5 % from the Sea of Galilee, ~12% from the Bitaniya effluents while the Brines water carrier provides ~73.5%. During the summer of 2001, the Degania dam was closed again and the relative contribution from each source had changed such the brines from the carrier account for most of the discharge. The differences in contribution of fluxes between winter and summer are illustrated in Figure 6.

Table 3: MCM results for Cell 1

Cell		Source		winter 00-01		summer 01	
				%cell inflow	% diff.	%cell inflow	% diff.
Cell_1	Alumot Bridge				2.56%		2.54%
		Cell_0	Outlet of Sea of Galilee	14.4	*	***	
		W.Surf.Inflow_121	Bitaniya	12.1		5.0	
		W.Surf.Inflow_122	Saline carrier	73.4		95.0	

Figure 6: Sources of water to the upper Jordan River (Cell 1) at Alumot dam: winter 2001 fluxes in blue and summer 2001 in yellow.

Cell 2: Beit Zera (1.3 km from Alumot) and Cell 3: Dalhamiya Bridge (5.6 km from Alumot)

The MCM model was performed for each cell (#2 at Beit Zera and #3 at Dalhamiah; Figure 7) to accommodate the winter 2001 records. For the summer of that year, however, due to lack of hydro-chemical data the MCM was performed for both cells 2 and 3 simultaneously. The location of the sampling point of Cells 2 and 3 are presented in Figure 7.

The possible sources to Cell-2 are the upstream cell-1 and the drainage of water from Dgania B. The chemical concentrations variations between the two cells, Cell-1 and Cell-2, are very slight. As it was expected, Cell 1 provides most of the water in the winter when the Degania dam was open. Results for Cell 2 (Table 4) show that effluents from W. Yavniel stream has a small role and it is account for ~7% in the winter and only ~2.3% in the summer. The discharge from the Sea of Galilee is the major contributor (~93%) during the winter and almost negligible (0%) during the summer. Most of the discharge into Cell 3 is from the upper stream cell (Cell 2). However, during the winter up to ~21.5% is contributed by the lateral drains from the cultivated nearby area. Small, yet significant contribution is noticeable from the Ashdot sewage treatment plant.

Cell-3 gets its flux from the upstream Cell-2 and from drained water by W.Drainage_208. The results show that W.Drainage_208 stops flowing during the summer time. The agricultural return flows mixed with natural saline groundwater constitutes the principal flow contribution to Cell-3 more up to 21% while the rest is from the upper reach of the river.

The increase in SO4 concentration (not in provenance of the two sources) suggests that there are other input flows (without data or unknown) to this cell. It is reflected by the water balance percentage difference (up to 4%).

Cell	Source		winter 00-01			summer 01		
			%cell inflow		% diff.	%cell inflow		% diff.
Cell_2 Beit Zera					3.89%			5.9%
	Cell_1		93.2			24.5		
	W.Surf.Inflow_123	W. Yavneal	6.8	**		0		
	W.Drainage_200	Degania b- kav tet 1		*		0		
Cell_3 Dalhamiya								
	Cell_2		78.6		7.30%			
	W.Drainage_201	Beit Zera - Cowshed		***			**	
	W.Drainage_202	Robed	0	*		0		
	W.Ground_203	Afikim - Groundwater		***			**	
	W.Drainage_204	Kelet -kav h		***			**	
	W.Drainage_205	Kochvani h1 (sewage)	0	*			**	
	W.Drainage_206	Point 121	0	*		0		
	W.Ground_207	Afikim - Groundwater		***			***	
	W.Drainage_208	kochvani	21.4	*		23.4		
	W.Drainage_209	Sha'ar		***			**	
	W.Drainage_210	Yarmuhim Reservoir	0	*		48.2		
	W.Drainage_211	Afikim		***		0		
	E.Surf.Inflow_400	Yarmouk River	0				***	
	W.Drainage_212	Point 110		***		0		
	W.Drainage_213	Ashdot waste		***		3.9		
	W.Drainage_214	Sephen Ashdot		***		0		
	W.Drainage_215	Zor- Ashdot		***		0		

Table 4: MCM results for Cells 2 and 3.

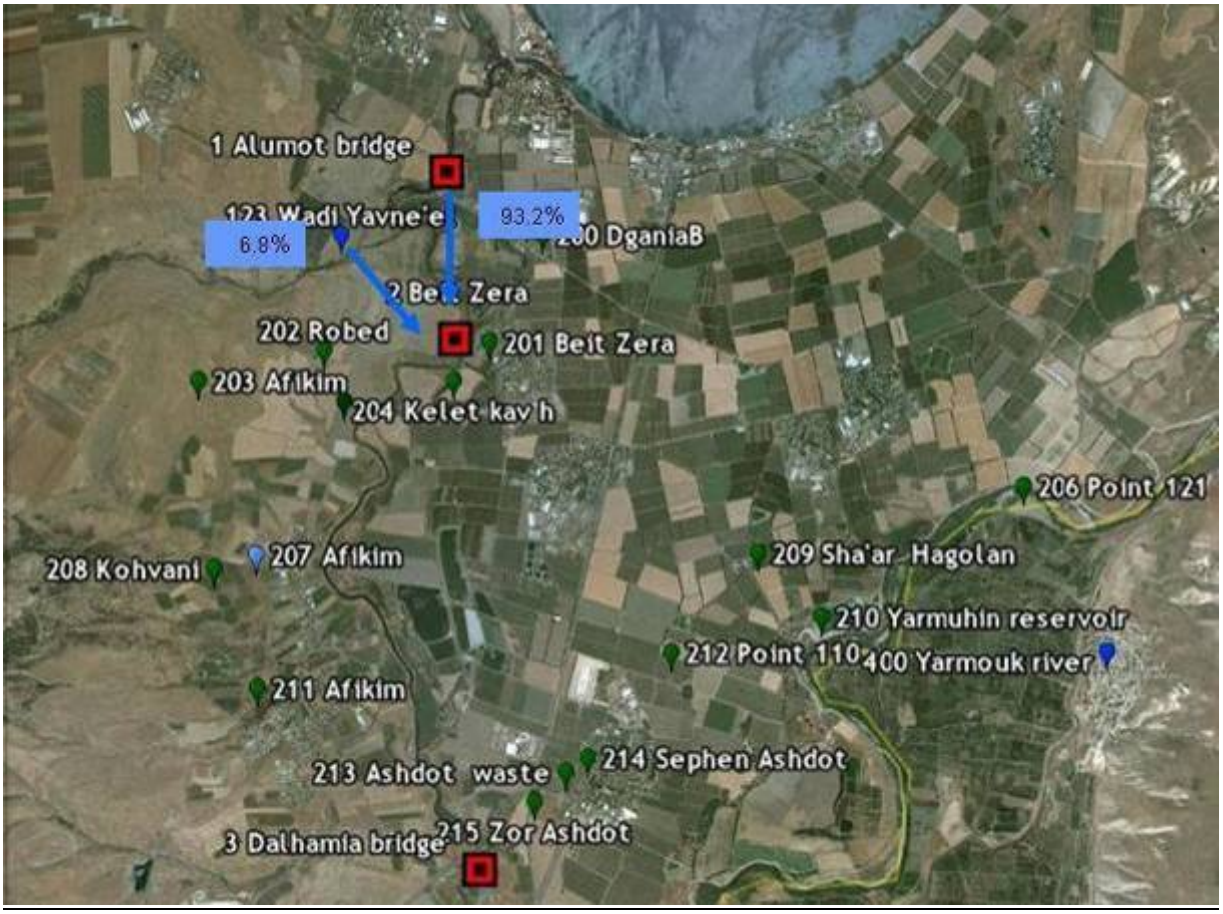

Figure 7: Sources of water to the upper Jordan River (Cell 2) at Beit Zera, winter 2001.

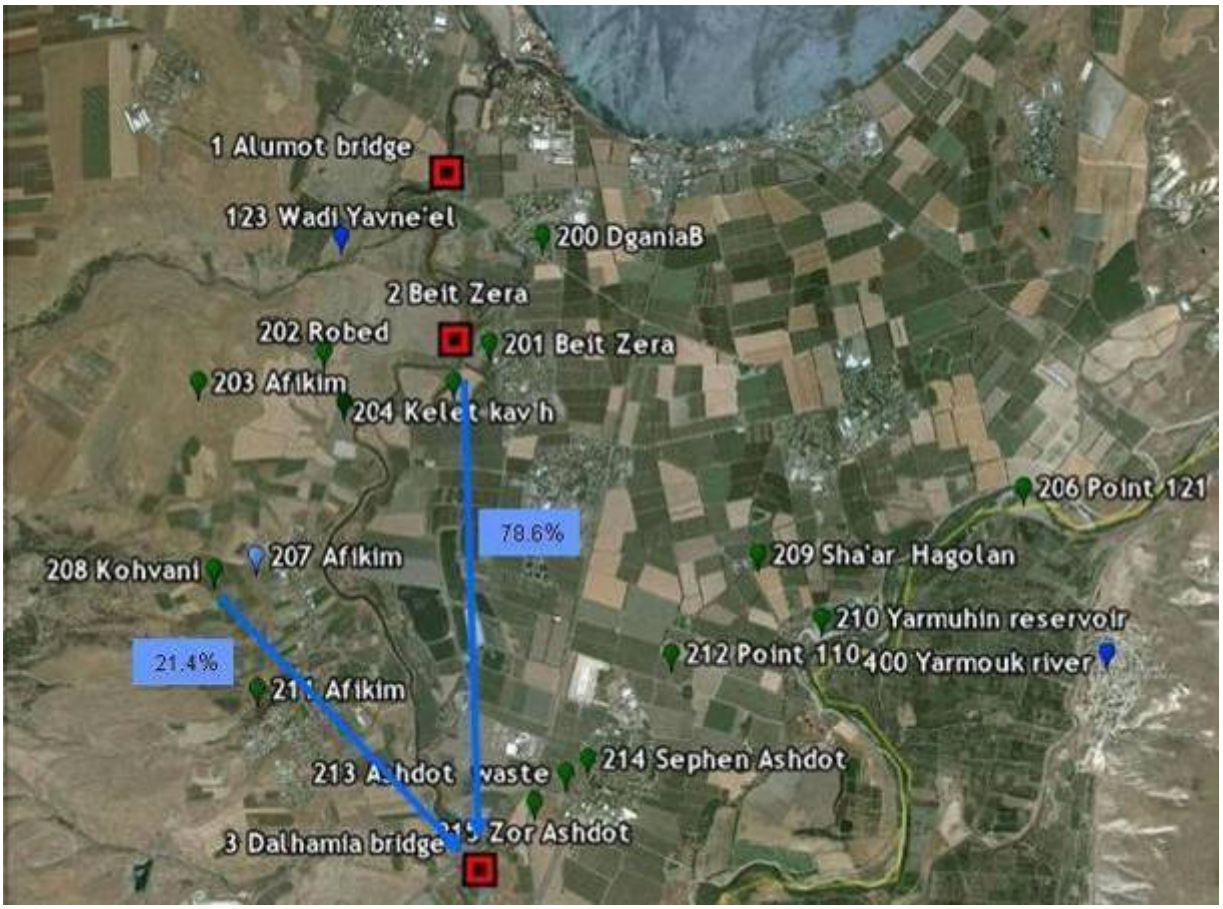

Figure 8: Sources of water to the upper Jordan River (Cell 3) at Dalhamiya, winter 2001.

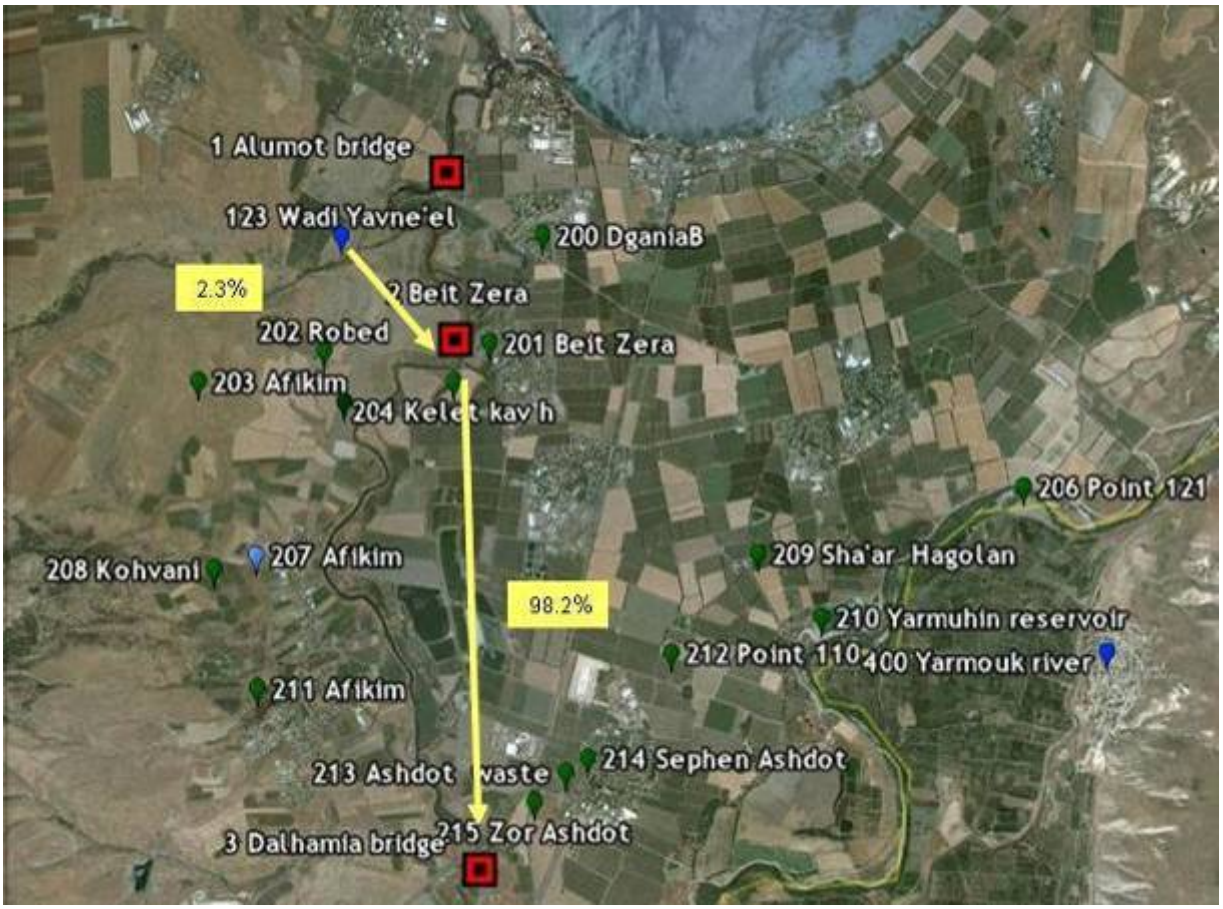

Figure 9: Sources of water to the upper Jordan River (Cell 3) at Dalhamiya, summer 2001.

Cell 4: Gesher (8.7 km from Alumot)

Most of the input to Cell 4 on the Jordan River at Gesher is from the upstream flow (from Cell-3) and, in addition, flows form the eastern tributary of the Yarmuk (at Naharyim; Figure 8). The Jordan River in Cell-3 at Al Dalhamiya Bridge and the Inflows from the Yarmuk at Naharaim have both lower Cl concentrations (and lower salinity) than the water salinity at Cell 4 (Gesher). Thereore, it is obvious than other sources (not yet identified and not included in this scenario) contribute to the salinity of this cell. The fluxes from the Yarmuk account for almost 25% of the discharge at Gesher in the winter (Table 5). It drops to almost 3% for the summer period when most of the Yarmuk flows are diverted into the Gohr Cannal for irrigation of the eastern Jordan Valley intensive agriculture. According to the results of the single cell model, these scenarios seem reasonable (with water balance percentage difference of less than 3.5%).

Cell	Source	winter 00-01		summer 01	
		%cell inflow	% diff.	%cell inflow	% diff.
Cell_4 Gesher			1.60%		3.32%
	Cell_3	77.3		97.2	
	W.Surf.Inflow_125 Yarmuok River - Naharayim	22.7		2.93	

Table 5: MCM results for Cell 4.

Figure 10: Sources of water to the upper Jordan River (Cell 4) at Gesher, winter 2001 fluxes in blue and summer 2001 in yellow.

Cell 5, N.Ur north (11.6 km from Alumot) and Cell 6, Neve Ur South (12.7 km from Alumot)

For the winter MCM modeling, Cell-5 at Neve Ur (north) is entirely alimented by the Jordan water flowing from the upstream cell (Cell 4; ~85%) and by groundwater seepage (represented by Bor_302 and Bor_303; ~14.5%).

Cell 6 receives its flow from the upstream cell Cell-5 while the distance between the two cells is only 1km. However, substantial inflows from Wade Arab

(E.Surf.Inflow_402) are expected (Figure 12). Missing summer samples (values) in the hydrochemical data base eliminated the water fluxes assessment for the summer period.

Results from winter 2001 (Table 6) indicate that flows from the upper cell (Neve Ur North accounted for about 66% and Wade Arab contributed less than 5% of the flux at Neve Ur South. Almost 30 % of the flows were originated by seepage of shallow groundwater and drains.

Cell		source		winter 00-01			summer 01		
				%cell inflow		% diff.	%cell inflow		% diff.
Cell_5	Neve Ur North					0.86%			3.25%
		Cell_4		85.7			5.4		
		W.Drain_126	Gesher drainage (81)		***		4.3		
		E.Well_451	Igam well		****			****	
		W.Bor_301	Borehole 1	0	*			***	
		W.Bor_302	Borehole 2	12.6	*		0.0		
		W.Surf.Inflow_127	N.Ur - Water canal (78)		***		1.0		
		W.Bor_303	Shaar 78	1.7	*		0.0		
Cell_6	Neve ur - South					1.02%			
		Cell_5		66.5					
		W.Bor_303	Shaar 78	0	*		0.0		
		W.Surf.Inflow_303	Shaar 78 River	0	*			***	
		W.FP_250	N.Ur pond		***		0.0		
		E.Surf.Inflow_401	North Shuna bridge(Wadi Arab water+thermal spring water)	3.8	*			***	
		E.Ground_452	North Shuna thermal	0	*			***	
		E.Surf.Inflow_402	Wadi Arab	0.9			0.0		
		W.Surf.Inflow_128	N.Ur - Water canal (76)		***		7.5		
		W.Surf.Inflow_129	N.Ur - Water canal (74)		***		55.0		
		W.Bor_304	Neve Ur South	28.9	*		26.7		

Table 6: MCM results for Cell 5 and Cell 6.

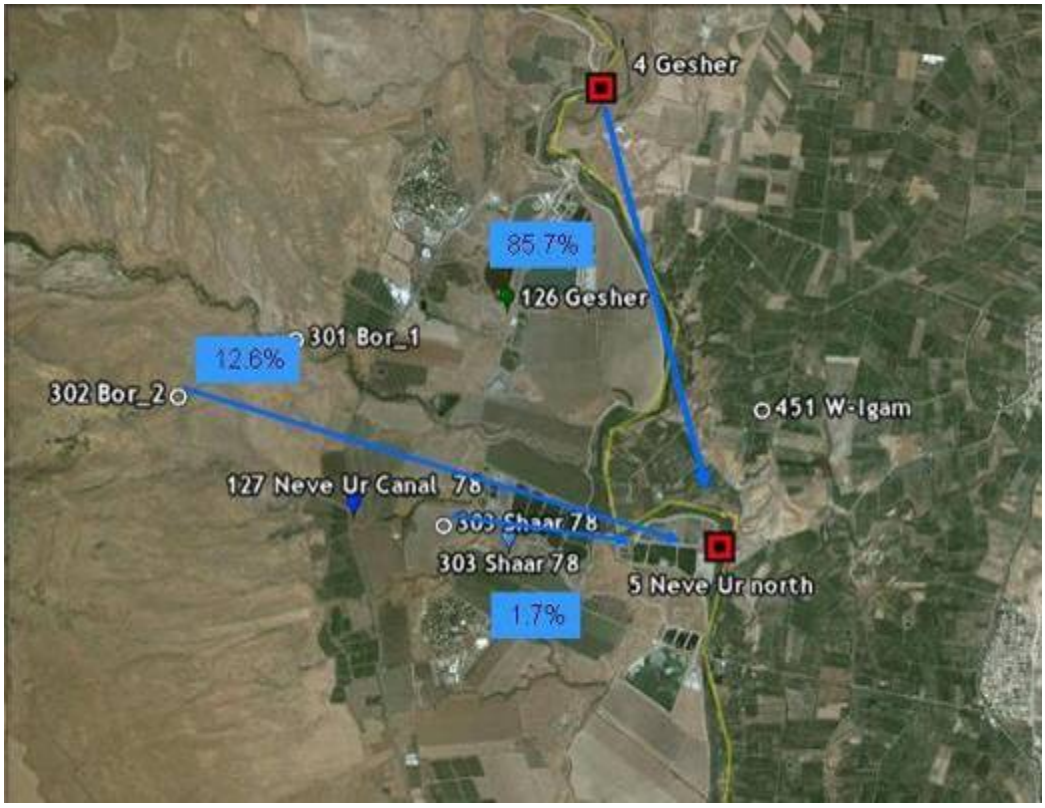

Figure 11: Sources of water to the upper Jordan River (Cell 5) at Neve Ur north, winter 2001.

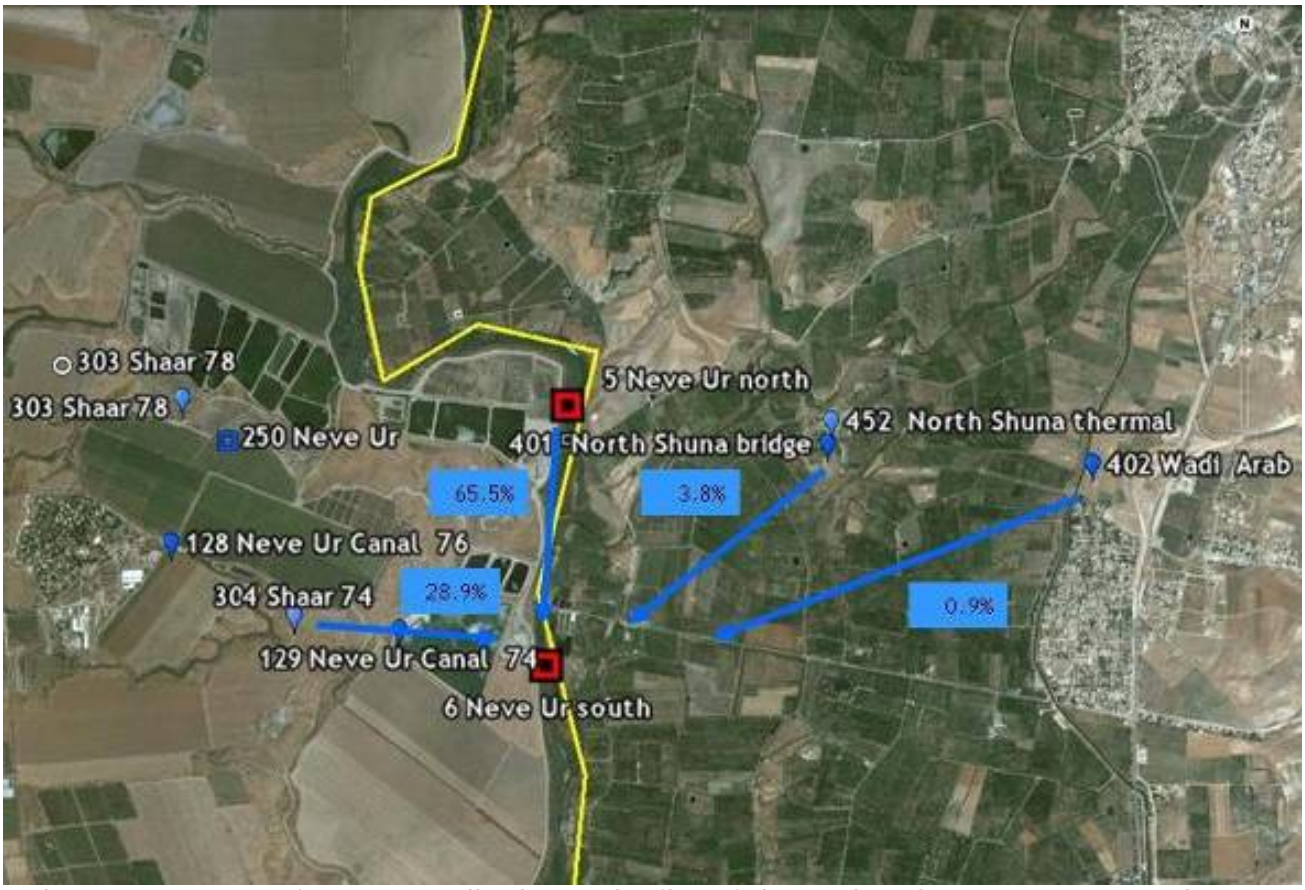

Figure 12: Sources of water contributing to the flux of the Jordan River at Neve-Ur South (Cell 6), winter 2001.

In the summer time groundwater seepage had been eliminated, replaced by substantial flow from the Neve Ur canal.

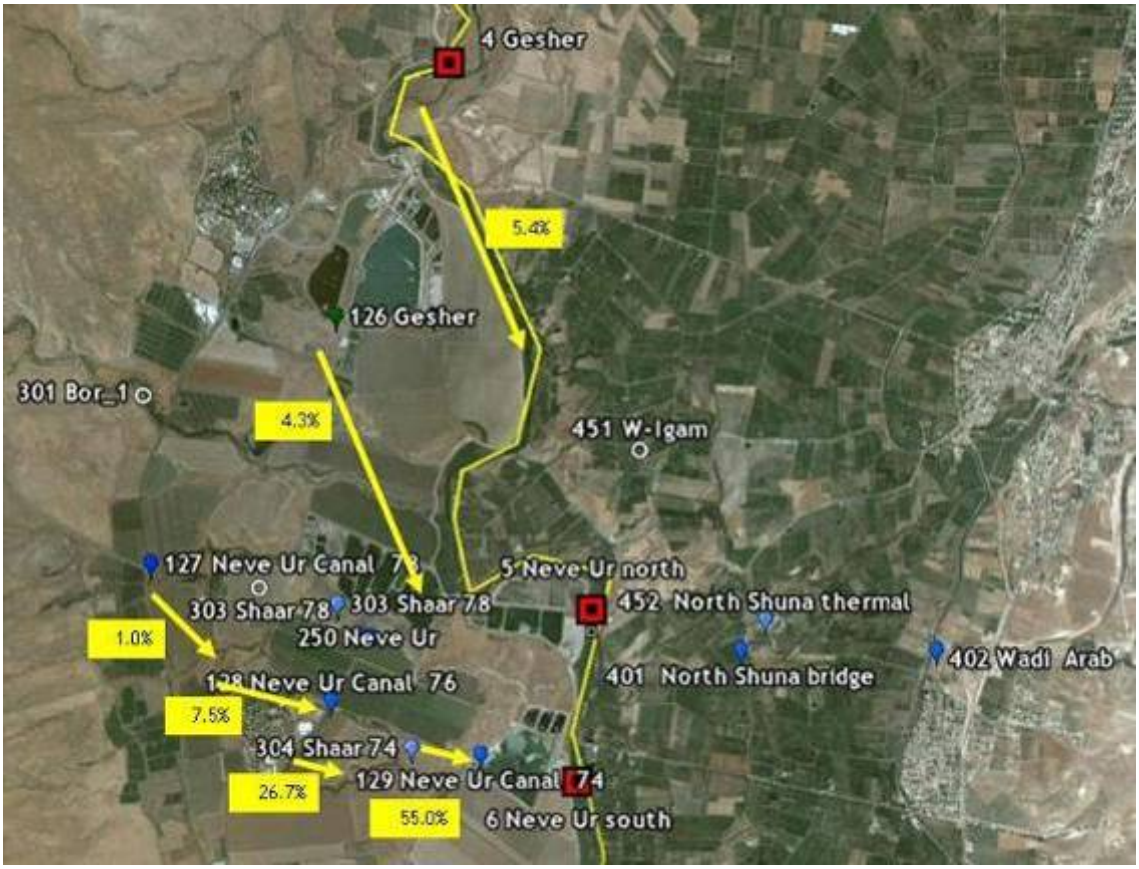

Figure 13: Sources of water contributing to the flux of the Jordan River at Neve-Ur South (Cell 6), summer 2001.

Cell 7: Hamadiya Pump North (Doshen; 18.6 km from Alumot), Cell 8: Hamadiya Pump South (Zor; 21 km from Alumot), Cell 9: G-48 (Gate 48 ; 21.6 km from Alumot) and Cell 10: Maoz Haim (22 km from Alumot)

The MCM model was applied simultaneously for the 2001 winter flows for Cells 7 and 8 and Cells 9 and 10, respectively (Table 7). The rest of the presented results are from single cell modeling approach aimed for detailed and rigorous assessment of all the active components contributing water and dissolved minerals to each segment along the river (Figure 10a). For winter 2001, inflows from the upper Jordan River report for ~92% of the flux at Hamadiya. About 8% is seepage of groundwater into the river. In Maoz Haim (Cell 10) about 42 % of the flux is from then upper Jordan River and 58% from runoff from the Harod River, a western tributary entering the Jordan River just north of Maoz Haim (Figure 10b). In Cell 7 alone, for the summer flow regime, about 50% of the flux passing by Hamadiya is originated by groundwater seepage (represented by boreholes W.Bor_308 and Hamadiya shallow well (W.Well_151). For the summer period, Cell 8 is mainly alimented by Hamadya fish ponds effluents. Further down in Maoz Haim, effluents from Canal 48 account for about 38% of the total discharge.

Cell		Source		winter 00-01			summer 01		
				%cell inflow		% diff.	%cell inflow		% diff.
Cell_7	Hamadiya pump -	North (doshen)				3.57%			7.61%
		Cell_6		92.2			49.1		
		E.Well_453	Fish F. well		**			***	
		W.Bor_308	Borehole 3	7.8	*		42.5		
		W.Bor_309	Gimel 73	0			0		
		W.Bor_310	Borehole 4	0			0.1		
		W.Bor_311	Borehole 5	0			1.4		
		E.Surf.Inflow_403	Wadi Teibeh	0			0		
		E.Surf.Inflow_404	Waqqas	0			0		
		W.Well_151	Hamadia - Well		***		7.9		
Cell_8	Hamadiya pump -	South (zor)							17.4%
		Cell_7			***		0		
		W.Bor_312	Borehole 6	0	*		0		
		W.Bor_313	Borehole 7	0	*		0		
		W.Bor_314	Shaar 56 Doshen	0	*		0		
		W.Surf.Inflow_130	Hamadiya - south canal		***		0		
		W.FP_251	Fish pond Hamadiya		***		100		
		W.Spring_454	Manshiya thermal	0	*			***	
		W.Bor_324	Canal 56 gimel		***		0		
		E.Well_455	Waqqas well		*			***	
Cell_9	g-48					5.05%			2.98%
		Cell_8		42			93.5		
		W.Ground_152	En Huga (Soda Station)		***		0	*	
		W.Spring_153	Hasida Spring		***		0	*	
		W.Surf.Inflow_131	Harod	58			6.5		
Cell_10	Maoz Haim								6.61%
		Cell_9			***		61.4		
		W.Surf.Inflow_132	Water canal 48		***		38.6		
		E.Surf.Inflow_405	Wadi Ziglab	0				***	

Table 7: MCM results for Cells 7, 8, 9 and 10.

Figure 14: Sources of water contributing to the flux of the Jordan River at Hamadiya North (Cell 7), summer 2001.

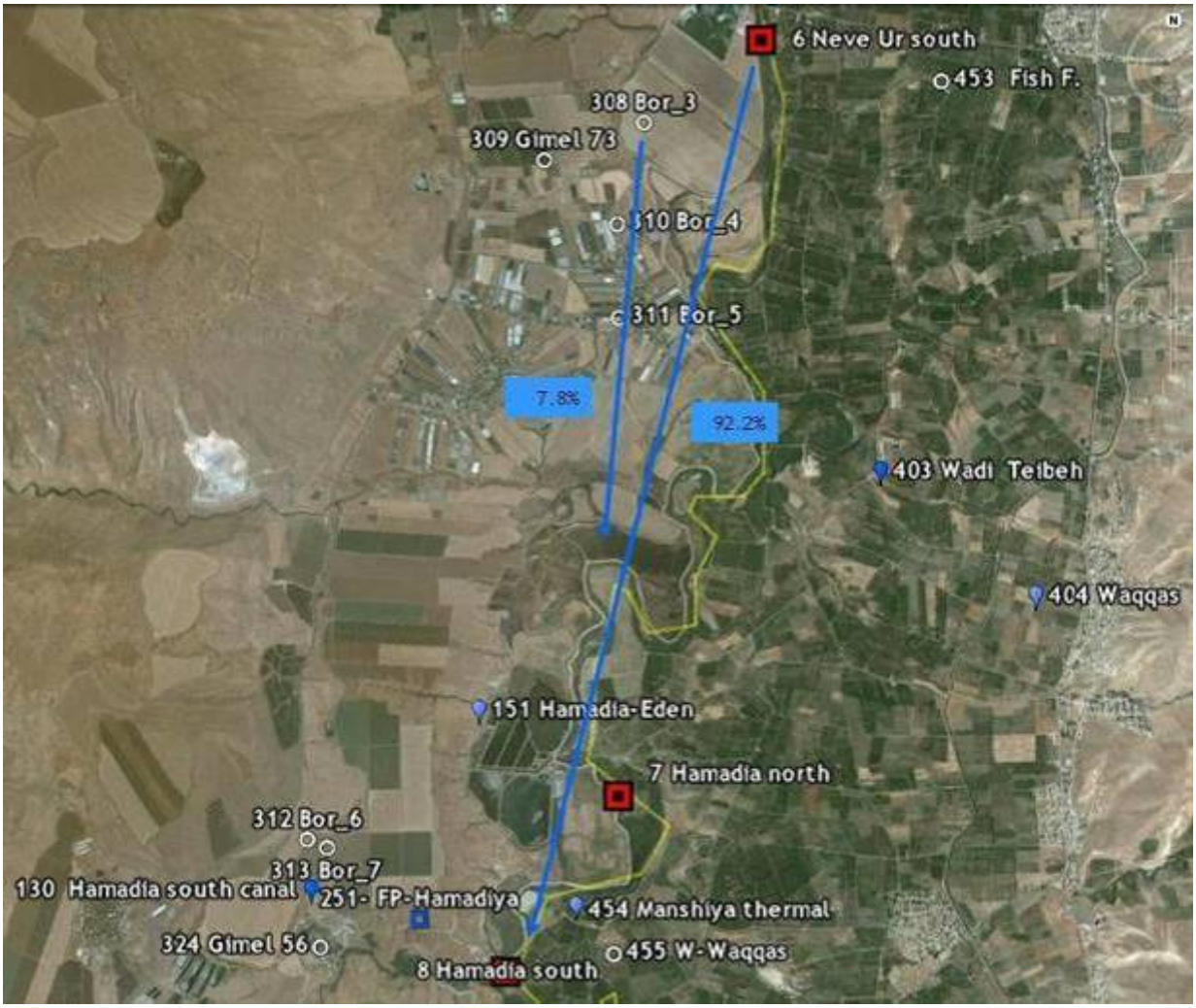

Figure 15: Sources of water contributing to the flux of the Jordan River at Hamadiya south (Cell 8), winter 2001.

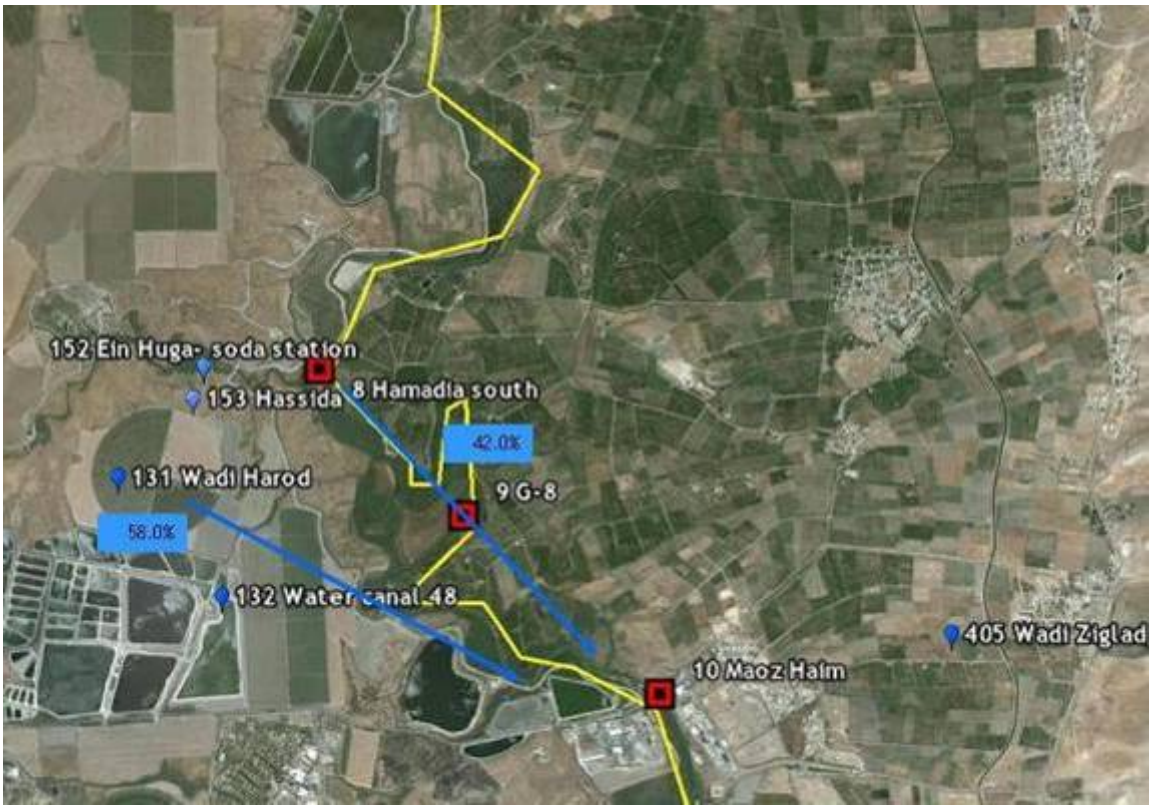

Figure 16: Sources of water contributing to the flux of the Jordan River at NeMaoz Haim (Cell 10), winter 2001 fluxes.

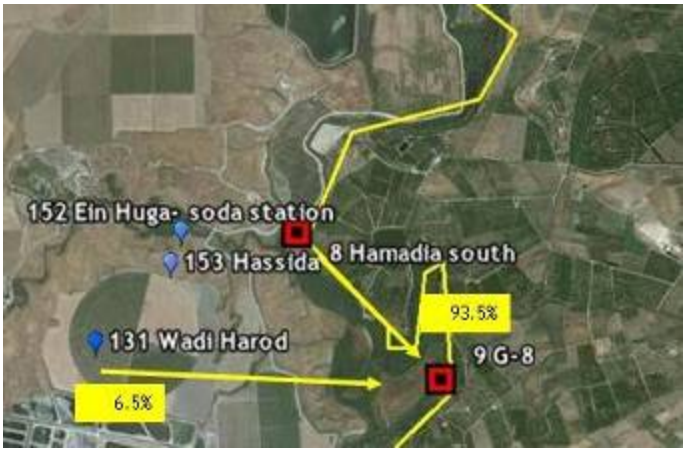

Figure 17: Sources of water contributing to the flux of the Jordan River at G-48 (Cell 9), summer 2001.

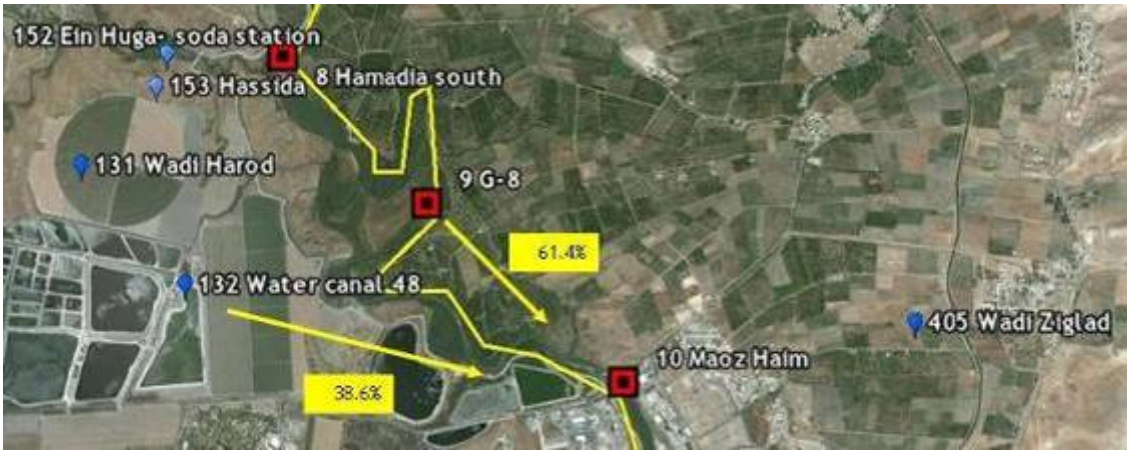

Figure 18: Sources of water contributing to the flux of the Jordan River at Maoz Haim (Cell 10), summer 2001.

Cells 11(Sheikh Hussein Bridge; 22.7 km from Alumot) and Cell 12 (Shifa Station; 27.7km from Alumot).

This segment of the Jordan River is characterized by the fact that winter and summer fluxes through both Sheikh Hussein Bridge and the Shifa Station (Figure 11) are generated entirely by surface flows either from the upper Jordan River or/and from Water Canal (W.Surf.Inflow_133; Table 8). Limited agriculture activities along this river reach explain the dry drains. The thick marl formations eliminate the seepage from shallow saline groundwater.

Cell		source		winter 00-01		summer 01	
				%cell inflow	% diff.	%cell inflow	% diff.
Cell_11	Sheich Husein Bridge				1.25%		4.14%
		Cell_10		88.8		24.5	
		W.Surf.Inflow_133	Water canal Nimrod	11.2		31.9	
Cell_12	Shifa' Station						
		Cell_11					
		E.Surf.Inflow_406	Abu Ziad	0		***	
		E.Surf.Inflow_407	Abu Thableh	0		***	
		W.Spring_456	Sp. unnamed	****		****	

Table 8: MCM results for Cells 11 and 12.

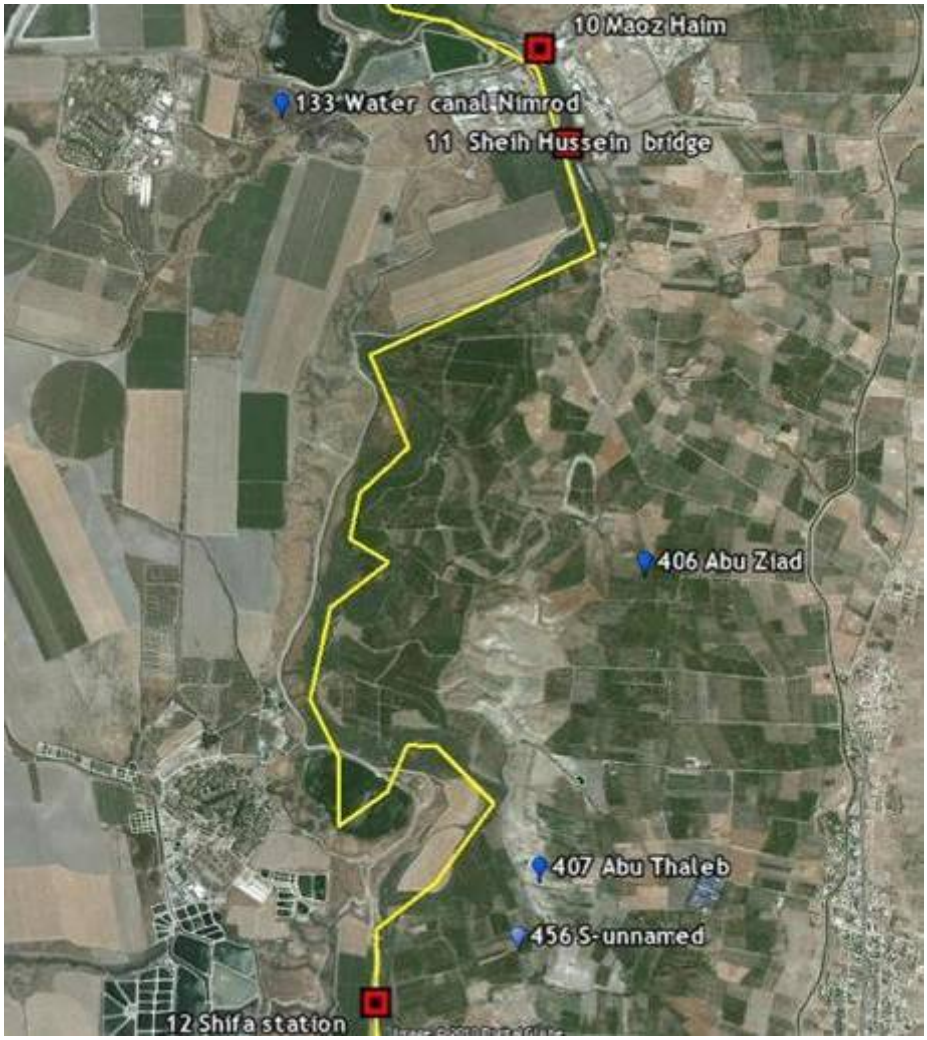

Figure 19: Sources of water contributing to the flux of the Jordan River at Sheikh Hussein Bridge (Cell 11) and at Shifa station (Cell 12).

Cells 13 (Gibton; 44 km from Alumot) and Cell 14 (Zarzir Station; 59.7km from Alumot).

The Jordan River along these two segments flow over massive marls formations, which eliminate any possible massive up-ward leakage from the regional aquifer. However, it is feasible to anticipate some lateral seepage from irrigation surplus form the cultivated area on both sides of the Jordan River. Also, many drains lead to canals

that discharge into the Jordan River. Many boreholes and drains were sampled (Figure 12) to characterize the chemical composition of the shallow groundwater over the marls over both banks of the river.

For the winter period, the MCM model was performed on Cells 13 (no data is avalaible for this period) and 14 simultaneously. For the summer time, each cell was individually assessed (Table 9).

In the winter period, about 55% of the discharge at Cell 14 through these cells is from the upper Jordan River. Almost 45% of the water is contributed from shallow groundwater and drains from the eastern bank of the basin (~10%). The obtained assessment for Cell 13 for summer 2001 is problematic due to un-acceptable water balance error, which has yet to be investigated. Results for Cell 14 indicate that the there is no contribution into the Jordan River from lateral seepage originated from shallow groundwater and drains. The later reflects the local hot climate and the limited irrigation toward the end of the growing season.

Cell		source		winter 00-01			summer 01		
				%cell inflow		% diff.	%cell inflow		% diff.
Cell_13	Gibton				***	3.76%			80.37%
		Cell_12		54.5			0		
		E.Surf.Inflow_408	Zoor Tbdulla	0				***	
		W.Spring_457	Abu thableh spring	24.5	*			***	
		E.Surf.Inflow_409	Masharie	0				***	
		E.Surf.Inflow_458	Mfadi well		****			****	
		E.Surf.Inflow_410	Mahrab Abu Ahm.		****			****	
		W.Spring_154	A-tin Spring		***				
		W.Spring_459	Juneidi Sp.		****			****	
		E.Well_460	Zenati F. well		****			****	
		W.FP_252	Tirat Zvi - pools		***			*	
		W.Spring_461	Sp. Unnamed		****			****	
		E.Surf.Inflow_411	Bassat Sharhabil		****			****	
		E.Surf.Inflow_412	Yabis	0				***	
		E.Surf.Inflow_413	Bassat Abu Habil		****			****	
		W.Spring_155	Sukot Spring	0			39.6	*	

		W.Surf.Inflow_134	Wadi el maliach	0				
		W.Spring_462	Qarn Sp.		****		****	
		W.Spring_463	Abu Namroud Sp.		****		****	
		E.Surf.Inflow_414	Kharoub	10.7			***	
		W.Bor_316	Borhole G-1	2.8	*	60.4	*	
		W.Bor_317	Borhole G-2	0.1	*		***	
		W.Bor_318	Borhole G-3	0	*		***	
Cell_14	Zarzir Station-58							27.60%
		Cell_13			***	98.1		
		W.Spring_464	Speera Sp.		***		***	
		E.Surf.Inflow_415	Bassat Abu Hamid	0		0		
		E.Surf.Inflow_416	Bassat Al Amira	0			***	
		W.Spring_465	Kufranja Sp.		***		***	
		E.Surf.Inflow_417	Rajib Seebiya	0		0		
		W.Spring_466	Faleh Sp.		***		***	
		E.Surf.Inflow_418	Bassat Faleh Wadi Botton	0		0		
		W.Spring_467	Buweib Sp.		***		***	
		E.Surf.Inflow_419	Bweib	0		0		
		E.Surf.Inflow_420	El Kheil		***	0		
		W.Spring_468	Kafir Sp.		***		***	
		E.Surf.Inflow_421	Kafir	3.21	*	0		
		W.Spring_469	Sp. unnamed		***		***	
		E.Surf.Inflow_422	Wadi Mikman	0		0		
		E.Surf.Inflow_423	Twal (west) Hawaya	0		0		
		E.Well_470	Deir Alla thermal well	0	*		***	
		E.Surf.Inflow_424	Mifshel	4.12		0		
		E.Surf.Inflow_425	Bassat Shakran	0		0		
		W.Surf.Inflow_135	Rafultzik-zarzir south		***	1.9		

Table 9: MCM results for Cells 13 and 14.

Figure 19: Sources of water contributing to the flux of the Jordan River at Gibton (Cell 13) and Zarzir Station (Cell 14).

Cells 15 (Adam Bridge; 66.4 km from Alumot), Cell 16 Tovlan; 72.4 km from Alumot), Cell 17 (Gilgal#107; 76.6 km from Alumot), Cell 18 (Alemby Bridge; 91 km from Alumot), Cell 19 (Baptism Site) and Cell 20 (Abdala Bridge)

Table 10 shows the MCM results obtained for the last five segments (compartments) assigned for the southern Jordan River. Due to massive water withdrawal from the upper Jordan basin, this reach of the river is often completely dry during both winter and the summer time. However, due to exceptional rainy season, the Jordan River carried perennial water all year around. The water sampling locations along the Jordan River and the location of the sampled boreholes are presented in Figure 13. The winter fluxes at the a Station (Cell 16) is entirely supported by runoff from the upper Jordan River (~80%) and from the eastern Zarka River (~20%) as can be depict from Table 10. During the summer time at the Adam Bridge (Cell 15) the groundwater portion in the total flux is estimated by ~10% (with very large water balance error ~17%!; Table 10), while the rest is related to flow coming from the upper Jordan River segments. The fluxes along Cells 17 are entirely originated from surface water from the upper Jordan and western streams during winter and summer without any significant contribution from other types of sources. Similar phenomenon was obtained for Cells 19 and 20 with small, yet significant seeping of groundwater (Table 10). The later probably reflects shallow water from the Jericho cultivated and irrigated area.

Cell		source		winter 00-01			summer 01		
				%cell inflow		% diff.	%cell inflow		% diff.
Cell_15	Adam Bridge					3.1%			16.98%
		Cell_14		80.3			90.3		
		W.Bor_315	Argaman swamp		***		9.7		
		E.Surf.Inflow_426	Zarqa River	18.6			0		
Cell_16	Tovlan Station - 83								3.10%
		Cell_15					96.9		
		W.Surf.Inflow_136	Tirtcha Upper				0		
		E.Surf.Inflow_427	Rasif				0		
		E.Bor_500	Damya Well no. 1	1.1	*		0		
		E.Surf.Inflow_428	Abu Mayyala				2.9		
		E.Surf.Inflow_429	Aqraa				0.2		
		E.Surf.Inflow_430	Mallah Gdeida				0		
		W.Ground_156	Tirtcha					***	
		E.Surf.Inflow_431	Qurein pool		***		0		
		W.Bor_321	Borhole T-2		*		0		
		W.Bor_322	Borhole T-3		*		0		
		W.Bor_323	Borhole T-4		*		0		
		W.Bor_320	Borhole T-1		*		0		
Cell_17	Gilgal - 107				***	92.30%			8.38%
		Cell_16		1.7			39.9		
		E.Surf.Inflow_432	Mallaha	0				****	
		W.Surf.Inflow_137	Tirtcha Lower	98.2			59.9		
		W.Surf.Inflow_138	Wadi el Ah'mar	0			0.2	*	
Cell_18	Alenby Bridge								
		Cell_17			***		99.6		22.56%
		E.Surf.Inflow_433	Bassat El Faras		**			***	
		E.Surf.Inflow_434	Wadi Mallaha Karama	0.1				***	
		W.Surf.Inflow_139	Uga Melecha		***		0		
		W.Ground_157	Uga Melecha		***		0.4		
Cell_19	Baptism site					2.09%			3.98%
		Cell_18		43.8			100		
Cell_20	Ab'dala Bridge								
		Cell_19		58.15			0		
		E.Well_471	Wadi Kafrain well	0	*			***	

	W.Well_158	Hagla - Well	1.16			***
	E.Well_472	Rama well	0	*		***
	E.Surf.Inflow_435	Kharar	0		0	
	E.Well_473	Hisban well	0	*		***
	E.Surf.Inflow_436	Hisban Kafrain	0		0	

Table 10. MCM results for Cells 15, 16, 17, 18, 19 and 20.

Figure 20: Sources of water contributing to the flux of the Jordan River at Adam Bridge (Cell 15), Tovlan Station (Cell 16), winter 2001.

Figure 21: Sources of water contributing to the flux of the Jordan River at Adam Bridge (Cell 15), summer 2001.

Figure 22: Sources of water contributing to the flux of the Jordan River at Tovlan Station (Cell 16), summer 2001.

Figure 23: Sources of water contributing to the flux of the Jordan River at Gilgal (Cell 17), at Allenby Bridge (Cell 18), at Baptism site (Cell 19) and at Abdallah bridge (Cell 20).

3.3 Results from the northern section of the Lower Jordan Valley: May and August 2001

The MCM *multi-cells* modeling approach was applied for simultaneous execution over the entire northern (and later to the southern) Jordan River segments with hydro-chemical data obtained during May and August 2001 water sampling campaigns. A MCM comprehensive modeling of the entire Lower Jordan River basin for these months failed due to lack of reliable data around Cells 50(Gibton)-51 (Zarzir Station) which imposed large water balance error.

Results which indicate the active sources and the relative fluxes in-between cells are given in the enclosed tables.

While the above single cells analyses were perform on average chemical and isotopic data for the winter (September 2000-February 2001) and summer (March 2001-August 2001), this analysis represent results from a single sampling tours (campaigns) performed in less than 10 days in May and August 2001, respectively. The schematic flow configuration among the compartments along the northern segment of the Jordan River is presented in Figure 24.

May-01

The unknown inflows are:

Cell		Source		Rate of	% of tot	% of cell
Id	Name	Id	Name	inflow	inflow	inflow
Cell 70	Alumot Bridge					
		IN-1	Sea of Galilee	0	0	0
		IN-2	Saline Carrier	12.56	16.2	98.2
		IN-3	Bitania	0.23	3	1.8
Cell 69	Beit Zera					
		D-5	Degania b	0.18	0.2	100
Cell 68	Dalhamiya Bridge					
		D-7	Kochvani h1	2.13	2.7	100
Cell 66	Naharayim					
		InJR-67	Yarmuok River - Naharayim	1.39	1.8	100

Cell 64	N.Ur north (78)					
		Bor-1		2.86	3.7	100
Cell 65	Neve ur - South					
		ES-14	Wadi El Arab	5.56	7.2	100
Cell 63	Hamadiya - North					
		Bor-4		1.68	2.2	30.5
		ES-14	Wadi El Arab	3.82	4.9	69.5
Cell 62	Hamadiya - South					
		ES-17	Waqqas	1.29	1.7	10.1
		FP-19	Hamadia - Eden	11.44	14.8	89.9
Cell 57	Maoz Haim					
		WS-23	Water Canal 48	14.7	19	100
Cell 53	Sheich Husein Bridge					
		WS-23	Water Canal 48	9.5	12.3	100
Cell 54	Shifa' Station					
		ES-25	Abu Ziad	3.22	4.2	100
Cell 50	Gibton					
		WS-SPRING	Sukot Spring	6.9	8.9	100

The intermediate flows are:

From cell		To cell		Rate of
Id	Name	Id	Name	flow
Cell70	Alumot Bridge	Cell69	Beit Zera	11.646
Cell69	Beit Zera	Cell68	Dalhamiya Bridge	12.003
Cell68	Dalhamiya Bridge	Cell66	Naharayim	12.838
Cell66	Naharayim	Cell64	N.Ur north (78)	12.837
Cell64	N.Ur north (78)	Cell65	Neve ur - South	16.565
Cell65	Neve ur - South	Cell63	Hamadiya - North	22.365
Cell63	Hamadiya - North	Cell62	Hamadiya - South	29.833
Cell62	Hamadiya - South	Cell57	Maoz Haim	44.446
Cell57	Maoz Haim	Cell53	Sheich Husein Bridge	62.209
Cell53	Sheich Husein Bridge	Cell54	Shifa' Station	75.096
Cell54	Shifa' Station	Cell50	Gibton	77.816

Total: 77.46 100.00 %

QOUT + PPP = 101.00

Absolute diff.: 23.54

Percentage diff.: 23.31 %

Table12: MCM results for Northern segment (''Segment One'', down to 66 km downstream from the Sea of Galilee), May 2001.

August-01

The unknown inflows are:

Cell		Source		Rate of	% of tot	% of cell
Id	Name	Id	Name	inflow	inflow	inflow
Cell 70	Alumot Bridge					
		IN-1	Sea of Galilee	0	0	0
		IN-2	Saline Carrier	15.56	17.1	94.4
		IN-3	Bitania	0.92	1	5.6
Cell 69	Beit Zera					

		D-5	Degania b	0.13	0.1	100
Cell 68	Dalhamiya Bridge					
		D-7	Kochvani h1	3.1	3.4	100
Cell 68A	Gesher					
		InJR-67	Yarmuok River - Naharayim	1.08	1.2	100
Cell 64	N.Ur north (78)					
		Bor-1		7.58	8.3	100
Cell 65	Neve ur - South					
		ES-14	Wadi El Arab	5.64	6.2	100
Cell 62	Hamadiya - South					
		ES-16	Wadi Teibeh	3.85	4.2	22.9
		ES-17	Waqqas	0.24	0.3	1.4
		WS-21	Hasida Spring	11.77	12.9	70
		BOR-4		0.94	1	5.6
Cell 54	Shifa' Station					
		WS-23	Water Canal 48	22.18	24.4	73.7
		ES-25	Abu Ziad	7.93	8.7	26.3
Cell 53	Sheikh Hussein Bridge					
		WS-27	Wadi el Maliach	0	0	0
Cell 51	Zarzir Station-58					
		ES-34	Hawwaya	0	0	0
		ES-35	Mifshel	10.2	11	100

The intermediate flows are:

From cell		To cell		Rate of flow
Id	Name	Id	Name	
Cell70	Alumot Bridge	Cell69	Beit Zera	15.647
Cell69	Beit Zera	Cell68	Dalhamiya Bridge	15.835
Cell68	Dalhamiya Bridge	Cell68A	Gesher	18.338
Cell 68A	Gesher	Cell64	N.Ur north (78)	17.817
Cell64	N.Ur north (78)	Cell65	Neve ur - South	22.426
Cell65	Neve ur - South	Cell62	Hamadiya - South	27.718
Cell 62	Hamadiya North	Cell54	Shifa' Station	45.915
Cell 54	Shifa station	Cell53	Sheikh Hussein Bridge	75.744
Cell 53	Sheikh Hussein Bridge	Cell51	Zarzir Station-58	83.984

Total: 90.96 100.00 %
QOUT + PPP = 101.00

Absolute diff.: 10.04
Percentage diff.: 9.94 %

Table13: MCM results for Northern segment (''Segment One'', down to 66 km downstream from the Sea of Galilee), August 2001.

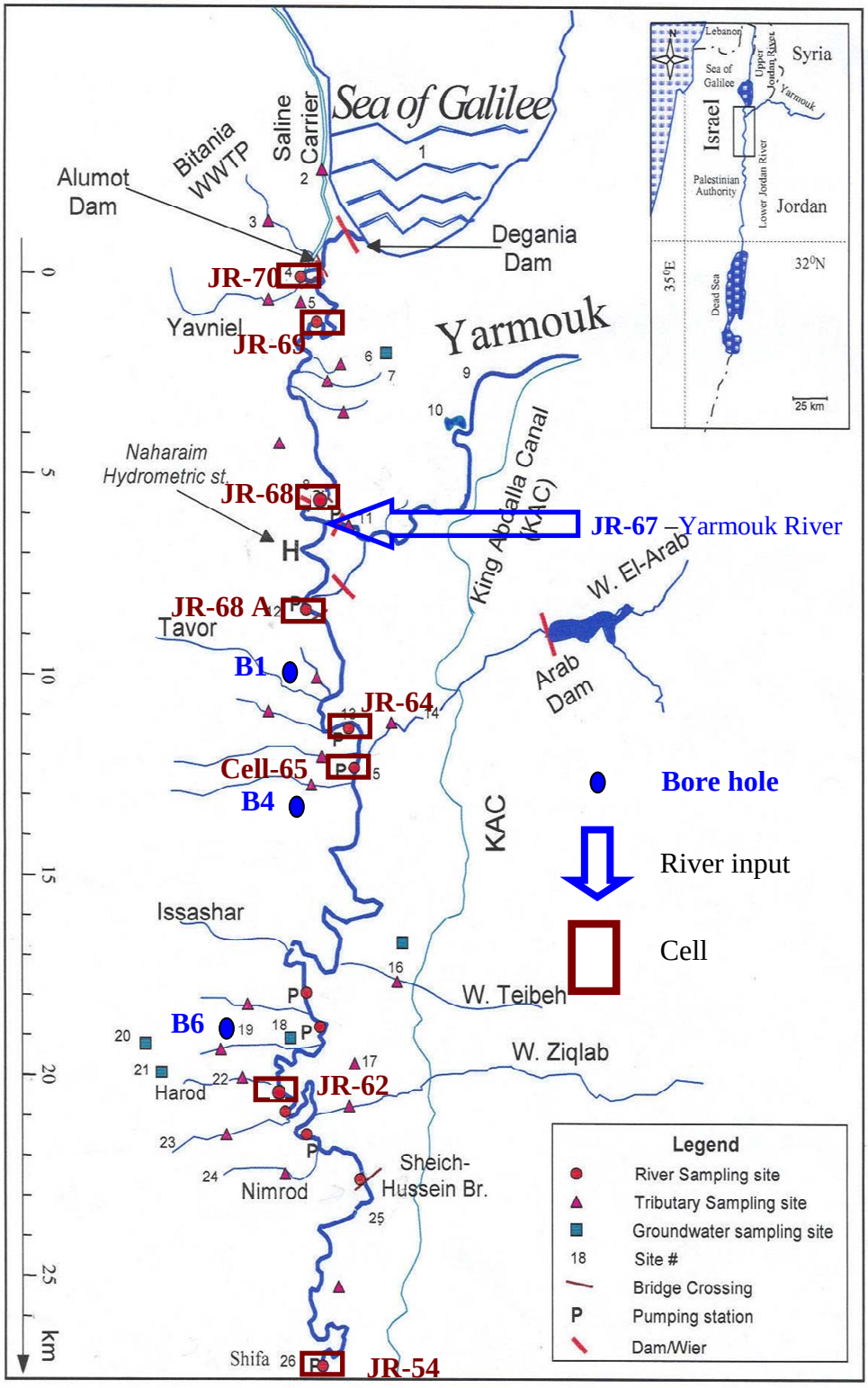

Figure 24. A schematic flow pattern among the cells along the northern segment of the Jordan River

3.4 Results from the southern section of the Lower Jordan Valley: May and August 2001

August 2001

The unknown inflows are:

Cell Id	Cell Name	Source Id	Source Name	Rate of inflow	% of tot inflow	% of cell inflow
Cell 49	Adam Bridge					
		Cell-51	Zarzir Station-58	81.6	79.5	92.7
		ES-37	Zarqa River	6.46	6.3	7.2
Cell 45	Gilgal - 107					
		ES-40	Rasif	0.61	0.6	4.4
		ES-41	Abu Mayyala	4.6	4.5	33
		ES-42	Aqraa	0.63	0.6	4.5
		ES-43	Mallah Gdeida	8.11	7.9	58.1
Cell 44	Zur el mandase					
		ES-42	Aqraa	0	0	0
		ES-45	Mallaha	0	0	0
		WS-48	Uga Melecha	0.11	0.1	100
Cell 42	Alenby Bridge					
		WS-46	Wadi el Ah'mar	0.57	0.6	100

The intermediate flows are:

From cell Id	From cell Name	To cell Id	To cell Name	Rate of flow
Cell 49	Adam Bridge	Cell 45	Gilgal - 107	85.92
Cell 45	Gilgal - 107	Cell 44	Zur el mandase	100.79
Cell 44	Zur el mandase	Cell 42	Alenby Bridge	103.11

Total: 102.69 100.00 %

QOUT + PPP = 101.00

Absolute diff.: 1.69

Percentage diff.: 1.68 %

Table14: MCM results for Lower segment (''Segment One'', down to 66 km downstream from the Sea of Galilee), August 2001.

May 2001

The unknown inflows are:

Cell		Source		Rate of	% of tot	% of cell
Id	Name	Id	Name	inflow	inflow	inflow
Cell 49	Adam Bridge					
		Cell-50	Gibton	20.52	21.3	57.6
		ES-29	Rajib Seebiya	0	0	0
		ES-34	Wadi Hawwaya	0.74	0.8	2.1
		ES-37	Zarqa River	14.37	14.9	40.3
Cell 47	Tovlan Station -83					
		WS-39	Tirtcha Upper	11.39	11.8	59.8
		ES-41	Abu Mayyala	4.92	5.1	25.8
		ES-42	Aqraa	0.23	0.2	1.2
		ES-43	Mallah Gdeida	2.51	2.6	13.2
Cell 45	Gilgal - 107					
		WS-46	Wadi el Ah'mar	0.2	0.2	100
Cell 44	Zur el mandase					
		ES-42	Aqraa	0.24	0.3	5.5
		ES-45	Mallaha	1.24	1.3	0
		WS-46	Wadi el Ah'mar	0	0	93.5
		WS-48	Uga Melecha	21.26	22	
Cell 42	Alenby Bridge					
		ES-45	Mallaha	1.05	1.1	5.6
		WS-48	Uga Melecha	17.85	18.5	94.4

The intermediate flows are:

From cell		To cell		Rate of
Id	Name	Id	Name	flow
Cell 49	Adam Bridge	Cell 47	Tovlan Station -83	34.08
Cell 47	Tovlan Station -83	Cell 45	Gilgal - 107	54.69
Cell 45	Gilgal - 107	Cell 44	Zur el mandase	56.8
Cell 44	Zur el mandase	Cell 42	Alenby Bridge	80.33

Total: 96.53 100.00 %

QOUT + PPP = 101.00

Absolute diff.: 4.47

Percentage diff.: 4.43 %

Table15: MCM results for Lower segment (‘‘Segment One’’, down to 66 km downstream from the Sea of Galilee), May 2001.

The results obtained by the MCM multi cells modeling approach are often different from that obtained for the same cells using the single cell approach. It reflects the differences in the hydro-chemical data set from each water sampling campaign, and that the optimization scheme is now performed with more chemical constraints. The differences in water balance for each cell or segment indicate the level of confidence of the results. High value of water balance difference suggest that the either the hydrologic setup deviates from the hydrological reality, or lack of accurate chemical and isotopic characteristics. It is used as a "red flag", suggesting alternative hydrological setup or refinement of the hydro-chemical data. In spite of the differences in absolute or relative calculated values, those sources that were selected by both *single* and *multi-cells* MCM approaches as contributors are positive definite sources that contribute water fluxes and dissolved solutes (minerals and/or dissolved contaminants) to the Jordan River in those particular segments.

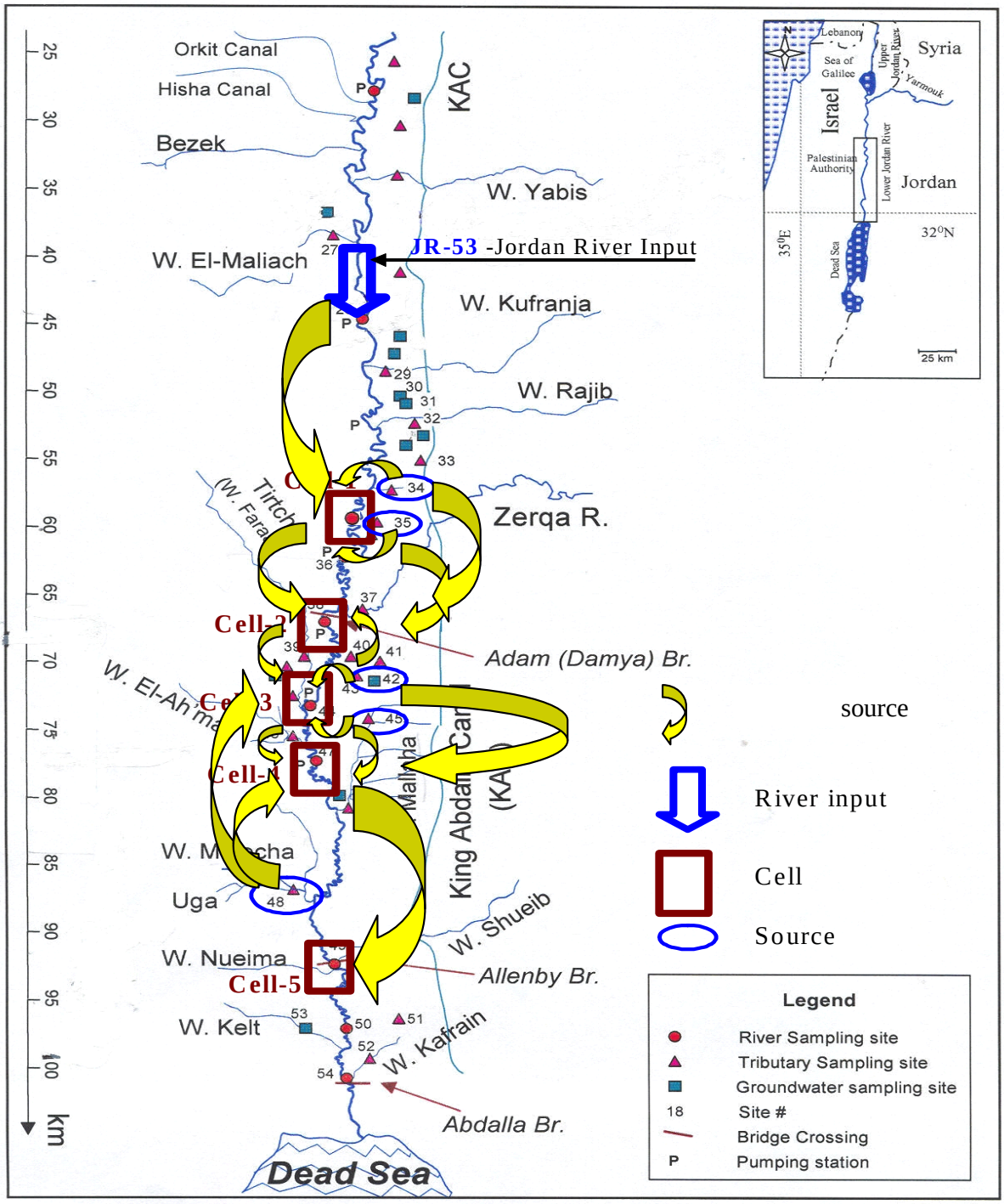

Figure 25. A schematic flow pattern among the cells along the southern segment of the Jordan River

4. Conclusions

This study evaluated the water quality dynamics along the Jordan River as a function of anthropogenic activities and natural processes by synthesizing existing hydrochemical data using Mixing Cell Modeling approach. A Comprehensive unified database including all the available chemical and hydrological data that exists for the Jordan River Basin was constructed and used to quantify the different water discharges and their qualities along the entire lower Jordan River. A clearer understanding of the active water resources contributing to the perennial stream of the Jordan River emerges from our modeling results. This includes the identification the role of Jordan River freshwater but mostly various contaminated sources that contribute to the current poor hydrochemical situation in the JRB. The existing hydrological conditions in the JRB resulted from the diversion of freshwater sources from the upstream catchment of the Jordan River (Sea of Galilee, Yarmuk and Zarka rivers) led to a reduction of the river flow into the Dead sea from about 1300 million cubic meters per year (MCM/yr) to about 30–200 MCM/yr. At the same time, water quality also deteriorated due to increase in anthropogenic activity (mainly due to discharge of wastewater and agriculture return flow), but also from natural saline water bodies.

The MCM model provides a tool for a quantitative assessment of all active sources into the Jordan River in every segment along the Lower Jordan Valley. It has been demonstrated that the MCM provides delicate hydrological tool for characterizing the variable water quality evolution along the complex Jordan River resulted by dynamic

behavior of the sources of recharge. Although the relative contribution of groundwater to the perennial stream is relatively low in winter time, this type of inflow is the major source for nutrients, fertilizers, herbicides and pesticides into the Jordan River. During the summer, however, when the discharge is smaller and the contribution of fresh water from the down-stream tributaries is diminished, the "role" and impact of the groundwater seepage on the Jordan water quality is even more significant and pronounced.

The presented modeling results also show that the main sources of marginal water to the JRB today are mainly: wastewater (untreated and treated to various levels), agriculture return flow, and saline shallow groundwater. The various sources of water carry different contaminants, which some of the impacts on the water quality and the environment is still largely unknown. The different sources of water show high spatial and temporal distributions. For example, in the northern parts of the basin, the main sources of marginal water flowing into the Jordan River are wastewater and agricultural return flow. As we move south, the contribution of saline shallow freshwater increases as compared to the wastewater and agricultural return flow. Although we anticipate that wastewater quality will generally improve in the next decade, it is unlikely that under the current situation the contribution of agricultural return flow will be reduced unless drastic measures will take place. In addition, seepage of saline shallow groundwater will continue to play a major role in the Jordan River hydro-ecological system. Aside of the upper Jordan, Yarmuk and Zarka inflows, no other major freshwater sources were identified during our work. It suggests that

identifying and exploiting deep groundwater reservoirs will have little effect (if any) on the Lower Jordan River water quality.

This study provides us with the scientific basis for a long-term research program to extend the evaluation of the water quality dynamics along the Jordan River as a function of anthropogenic activities and natural processes. The gaps in available information that was discovered and presented here could be obtained to provide the missing information needed to come up with solid strategies for sustainable remediation and development of the Jordan River Basin. These results can now serve as solid foundations to investigate the evolution of the aquatic ecology along every segment of the Jordan River as the bio-mass of fauna and flora are extremely sensitive to the temporal variations of the dissolved minerals and organic compounds. It also provided a firm basis for the future river ecosystem rehabilitation opportunities as part of the development of the JRB. Finally, we see here an excellent opportunity to generate a long-term partnership between researchers at both sides of Jordan River Basin, since the enormous task of managing and solving problems related to cross-border water resources requires also synergistic collaboration of young scientists from both side of the Jordan River.

5. References

1. Abu-Jaber, N., & Ismail, M. (2003). Hydrogeochemical modeling of the shallow groundwater in the northern Jordan Valley. Environmental Geology, 44(4), 391-399.

2. Adar, E., Rosenthal, E., Issar, A. S., & Batelaan, O. (1992). Quantitative assessment of flow pattern in the southern Arava Valley (Israel) by environmental tracers in a mixing cell model. Journal of Hydrology, 136, 333-354.

3. Adar, E., & Sorek, S. (1989). Multi-Compartmental Modeling for Aquifer Parameter-Estimation Using Natural Tracers in Non-Steady Flow. Advances in Water Resources, 12(2), 84-89.

4. Adar, E. M., & Neuman, S. P. (1988). Estimation of Spatial Recharge Distribution Using Environmental Isotopes and Hydrochemical Data .2. Application to Aravaipa Valley in Southern Arizona, USA. Journal of Hydrology, 97(3-4), 279-302.

5. Adar, E. M., Neuman, S. P., & Woolhiser, D. A. (1988). Estimation of Spatial Recharge Distribution Using Environmental Isotopes and Hydrochemical Data .1. Mathematical-Model and Application to Synthetic Data. Journal of Hydrology, 97(3-4), 251-277.

6. Al-Jayyousi, O., & Bergkamp, G. (2008). Water Management in the Jordan River Basin: Towards an Ecosystem Approach (pp. 105-121).

7. Al Kuisi, M., Aljazzar, T., Rude, T., & Margane, A. (2008). Impact of the Use of Reclaimed Water on the Quality of Groundwater Resources in the Jordan Valley, Jordan. Clean-Soil Air Water, 36(12), 1001-1014.

8. Anker, Y., Rosenthal, E., Shulman, H., & Flexer, A. (2009). Multi-disciplinary modeling, in stratigraphy and groundwater stratigraphy of the Jordan River basin. [10.1007/s00254-008-1335-8]. Environmental Geology, 57(2), 275-283.

9. Barel-Cohen, K., Shore, L. S., Shemesh, M., Wenzel, A., Mueller, J., & Kronfeld-Schor, N. (2006). Monitoring of natural and synthetic hormones in a polluted river. Journal of Environmental Management, 78(1), 16-23.

10. Farber, E., Vengosh, A., Gavrieli, I., Marie, A., Bullen, T. D., Mayer, B., et al. (2004). The origin and mechanisms of salinization of the Lower Jordan River. Geochimica Et Cosmochimica Acta, 68(9), 1989-2006.

11. Farber, E., Vengosh, A., Gavrieli, I., Marie, A., Bullen, T. D., Mayer, B., et al. (2005). Management scenarios for the Jordan River salinity crisis. Applied Geochemistry, 20(11), 2138-2153.

12. Farber, E., Vengosh, A., Gavrieli, I., Marie, A., Bullen, T. D., Mayer, B., et al. (2007). The geochemistry of groundwater resources in the Jordan Valley: The impact

of the Rift Valley brines. [doi: DOI: 10.1016/j.apgeochem.2006.12.002]. Applied Geochemistry, 22(3), 494-514.
13. Holtzman, R., Shavit, U., Segal-Rozenhaimer, M., Gavrieli, I., Marei, A., Farber, E., et al. (2005). Quantifying ground water inputs along the Lower Jordan River. [Article]. Journal of Environmental Quality, 34(3), 897-906.
14. Moller, P., Rosenthal, E., Geyer, S., Guttman, J., Dulski, P., Rybakov, M., et al. (2007). Hydrochemical processes in the lower Jordan valley and in the Dead Sea area. Chemical Geology, 239(1-2), 27-49.
15. Rosenthal, E., Guttman, J., Sabel, R., & Moller, P. (2009). Limiting hydrochemical factors for sustainability of water resources: The Cisjordanian experience. Chemie Der Erde-Geochemistry, 69(3), 191-222.
16. Salameh, E., & Naser, H. (1999). Does the actual drop in Dead Sea level reflect the development of water resources within its drainage basin? Hydrochim. Hydrobiol. Acta 27, 5-11.
17. Segal-Rozenhaimer, M., Shavit, U., Vengosh, A., Gavrieli, I., Farber, E., Holtzman, R., et al. (2004). Sources and transformations of nitrogen compounds along the Lower Jordan River. Journal of Environmental Quality, 33(4), 1440-1451.